

Competitive Desulfonylative Reduction and Oxidation of α -Sulfonylketones Promoted by Photoinduced Electron Transfer with 2-Hydroxyaryl-1,3-dimethylbenzimidazolines under Air

Eietsu Hasegawa,* Shyota Nakamura, Kazuki Oomori, Tsukasa Tanaka, Hajime Iwamoto, and Kan Wakamatsu

Cite This: *J. Org. Chem.* 2021, 86, 2556–2569

Read Online

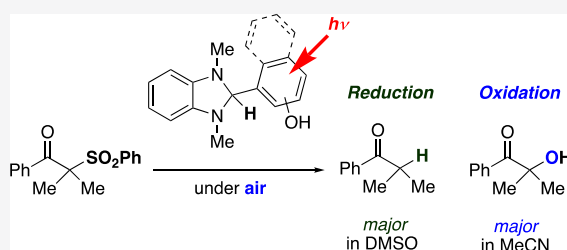
ACCESS |

Metrics & More

Article Recommendations

Supporting Information

ABSTRACT: Desulfonylation reactions of α -sulfonylketones promoted by photoinduced electron transfer with 2-hydroxyarylbenzimidazolines (BIH-ArOH) were investigated. Under aerobic conditions, photoexcited 2-hydroxynaphthylbenzimidazole (BIH-NapOH) promotes competitive reduction (forming alkylketones) and oxidation (producing α -hydroxyketones) of sulfonylketones through pathways involving the intermediacy of α -ketoalkyl radicals. The results of an examination of the effects of solvents, radical trapping reagents, substituents of sulfonylketones, and a variety of hydroxyaryl- and aryl-benzimidazolines (BIH-ArOH and BIH-Ar) suggest that the oxidation products are produced by dissociation of α -ketoalkyl radicals from the initially formed solvent-caged radical ion pairs followed by reaction with molecular oxygen. In addition, the observations indicate that the reduction products are generated by proton or hydrogen atom transfer in solvent-caged radical ion pairs derived from benzimidazolines and sulfonylketones. The results also suggest that arylsulfinate anions arising by carbon-sulfur bond cleavage of sulfonylketone radical anions act as reductants in the oxidation pathway to convert initially formed α -hydroperoxyketones to α -hydroxyketones. Finally, density functional theory calculations were performed to explore the structures and properties of radical ions of sulfonylketones as well as BIH-NapOH.



INTRODUCTION

Reduction and oxidation (redox) reactions often occur through single electron transfer (SET)-promoted pathways.¹ Typically, visible or UV light irradiation is utilized to induce SET-promoted redox reactions, termed photoinduced electron transfer (PET), by supplying energy to the electron donor or acceptor to facilitate SET.² While investigations of PET reactions of organic molecules have a long history,² some noteworthy recent advancements have been made in developing synthetic applications of these photoredox processes through the use of transition-metal complexes and nonmetal containing substances as visible light-absorbing photocatalysts.^{3,4} In these reactions, stoichiometric amounts of appropriate co-operating materials are usually required to promote the conversion of substrates and regeneration of photocatalysts. For example, dihydropyridines such as Hantzsch esters are frequently employed for this purpose in photocatalyzed reduction reactions of organic substrates.⁵ Although less explored, organic electron-donating substances, which absorb visible light, can be employed as photoexcited reductants operating without using photocatalysts.^{6,7}

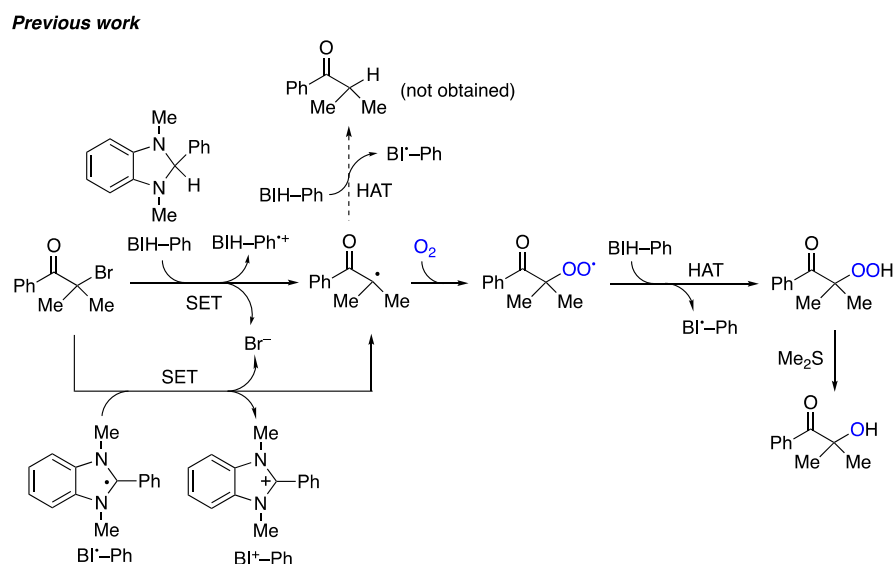
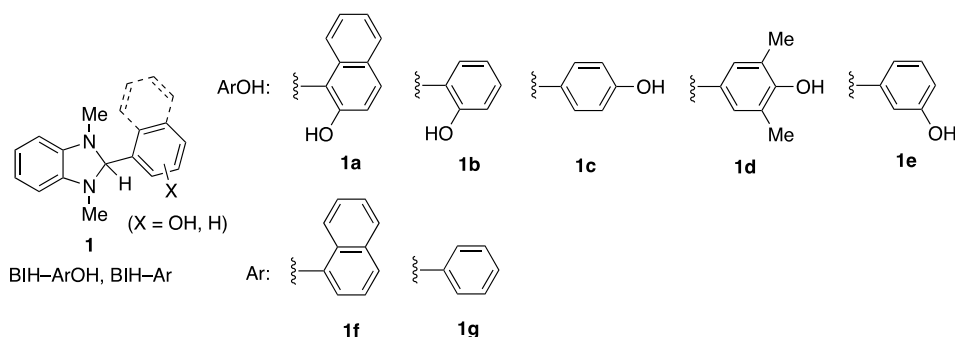
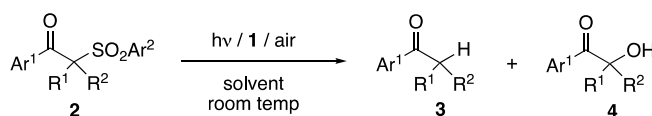
2-Aryl-1,3-dimethylbenzimidazolines (BIH-Ar) and 2-hydroxyaryl-1,3-dimethylbenzimidazolines (BIH-ArOH), which are recognized as artificial nicotinamide adenine dinucleotide analogues and serve as electron as well as hydrogen atom

donors,⁸ have been utilized in various chemical processes.^{9–16} In several past investigations of PET reactions of various organic substances,¹⁷ we demonstrated that photoexcited BIH-Ar and BIH-ArOH can be employed to promote reduction of organic substrates.¹⁸ In addition, we demonstrated that the oxidized form of BIH-ArOH, BI⁺-ArO⁻, acts as unprecedented visible light-absorbing betaine photocatalysts.¹⁹ Recently, we found that the strong electron-accepting substrate, α -bromoisobutyrophenone [$E_{1/2}^{\text{red}} = -1.15$ V vs saturated calomel electrode (SCE)], reacts with 1,3-dimethyl-2-phenylbenzimidazole (BIH-Ph) to promote exclusive α -hydroxyketone forming reaction under the aerobic conditions without the use of heat, light, and catalysts (Scheme 1).²⁰ In this process, initial SET from BIH-Ph to the bromoketone induces loss of bromide ion to generate an α -ketoalkyl radical, which is subsequently trapped by molecular oxygen followed by hydrogen atom transfer (HAT) to give α -hydroperoxyisobutyrophenone and

Received: November 9, 2020

Published: January 25, 2021



Scheme 1. SET and HAT Pathways for Debrominative Oxidation of α -Bromoisobutyrophenone Promoted by 1,3-Dimethyl-2-phenylbenzimidazoline (BIH-Ph) under Air**This work**~ Photoexcited benzimidazolines **1** (BIH-ArOH and BIH-Ar) ~~ Desulfonylative hydrogenation and oxygenation of α -sulfonyl ketones **2** ~

- 2a** Ar¹ = Ph, Ar² = Ph, R¹ = R² = Me
2b Ar¹ = Ph, Ar² = Ph, R¹ = PhCH₂, R² = H
2c Ar¹ = Ph, Ar² = Ph, R¹ = R² = H
2d Ar¹ = *p*-MeC₆H₄, Ar² = Ph, R¹ = R² = Me
2e Ar¹ = *p*-ClC₆H₄, Ar² = Ph, R¹ = R² = Me
2f Ar¹ = Ph, Ar² = *p*-MeC₆H₄, R¹ = R² = Me
2g Ar¹ = Ph, Ar² = *p*-MeOC₆H₄, R¹ = R² = Me

Figure 1. PET-promoted desulfonylative reduction and oxidation of α -sulfonyl arylketones **2** by using photoexcited benzimidazolines **1** under air.

benzimidazolyl radical (BI[•]-Ph). Moreover, exergonic SET from the formed BI[•]-Ph to the bromoketone followed by bromide ion loss yields the α -ketoalkyl radical and benzimidazolium cation ($E_{1/2}^{\text{red}} = -1.61$ V vs SCE). Finally, hydroperoxyketone obtained after a work-up operation is reduced by using Me₂S to produce α -hydroxyisobutyrophenone.

The earlier observations described above motivated us to carry out a detailed investigation of processes in which α -

ketoalkyl radicals are generated under aerobic PET conditions using BIH-Ar or BIH-ArOH. In particular, we were interested in assessing the relevance of earlier suggestions that PET-generated carbonyl radical anions and radical cations of amines possessing α -hydrogens undergo proton transfer (PT) within contact (solvent-encased) radical ion pairs²¹ and that radical ions and radical intermediates are captured by molecular oxygen only after their dissociation from solvent cages.²² Specifically, we anticipated that BIH-Ar and BIH-ArOH

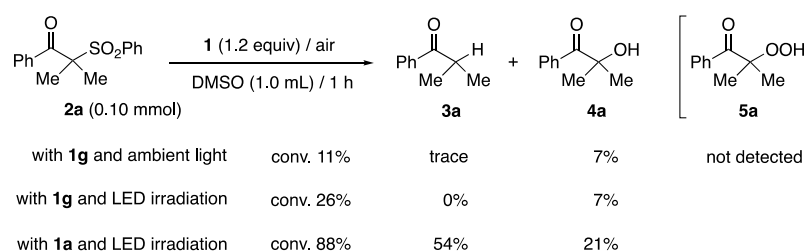
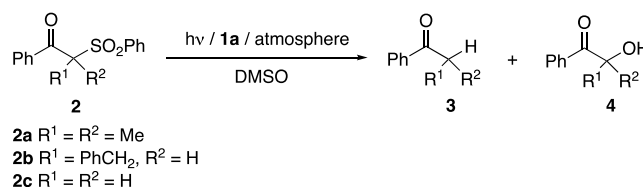


Figure 2. Reactions of α -phenylsulfonylisobutyrophenone **2a** and phenylbenzimidazoline **1g** with or without LED irradiation or hydroxynaphthylbenzimidazoline **1a** with LED irradiation under air. Conversion of **2a** and yields of **3a** and **4a** were determined by ^1H NMR.

Table 1. Photoreactions of α -Sulfonylphenones **2a–c** with Hydroxynaphthylbenzimidazoline **1a** under Different Atmospheric Conditions^a



entry	2	atmosphere	irrad time (h)	conv of 2 (%) ^b	yields (%) ^b		ratio (%)	
					3	4	3	4
1	2a	O ₂	4	100	43	39	52	48
2	2a	air	4	100	65 [57] ^c	23 [24] ^c	74 [70]	26 [30]
3	2a	N ₂	4	100	85	0	100	0
4	2b	O ₂	1	85	65	20	76	24
5	2b	air	1	100	78	20	80	20
6	2b	N ₂	1	100	98	0	100	0
7	2c	O ₂	1	100	49	0	100	0
8	2c	air	1	100	86	0	100	0
9	2c	N ₂	1	100	89	0	100	0

^a2 (0.10 mmol), **1a** (1.2 equiv vs 2), DMSO (1.0 mL), 7.3 W white LED. ^bDetermined by using ^1H NMR. ^cIsolated by using column chromatography.

promoted PET reactions of α -heterosubstituted ketones, which have appropriately tuned electron-accepting properties,²³ would take place via pathways in which ketone radical anions or α -ketoalkyl radicals undergo proton or hydrogen atom abstraction (reduction pathway) from BIH-Ar^{•+} or BIH-ArOH^{•+} within contact radical ion pairs (CRIPs). Furthermore, we expected that under aerobic conditions these radical intermediates would react with molecular oxygen (oxidation pathway) following their diffusion from CRIPs. In the study described below, which has provided affirmative information about these proposals, we examined competitive desulfonylative reduction and oxidation reactions of α -sulfonylketones **2** promoted by photoexcited benzimidazolines **1** under aerobic conditions (Figure 1; also see Figures S1 and S2).²⁴

RESULTS AND DISCUSSION

In the initial phase of this effort, we explored reactions of α -phenylsulfonylisobutyrophenone (**2a**) ($E_{1/2}^{\text{red}} = -1.66$ V vs SCE, see Figure S3 and Table S1) promoted by 2-hydroxyaryl-1,3-dimethylbenzimidazoline (**1a**) and 1,3-dimethyl-2-phenylbenzimidazoline (**1g**) (Figure 2). Reaction of **2a** with **1g** was first conducted under the conditions [dimethyl sulfoxide (DMSO), room temperature, air atmosphere] which would have led to complete conversion of α -bromoisobutyrophenone to the corresponding α -hydroperoxyphenone **5a** (see Scheme 1).²⁰ However, ^1H NMR analysis of the product mixture showed that this process generates a trace of isobutyrophenone **3a** and

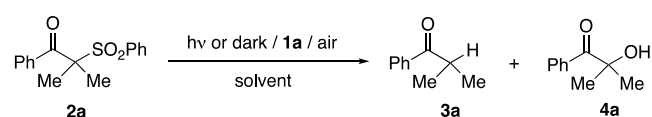
only a small quantity of α -hydroxyisobutyrophenone **4a**. This observation clearly suggests that **2a** and **1g** do not efficiently participate in a dark SET–HAT reaction, like the one occurring between α -bromoisobutyrophenone and **1g** (see Scheme 1). Irradiation of these reactants using a 7.3 W white light emitting diode (LED) increased the conversion of **2a** to some extent but the yield of **4a** is still low. In contrast, reaction of **2a** does take place to form **3a** as well as **4a** (85% mass balance) when **1a** along with visible light irradiation using the same LED are employed.

These preliminary observations encouraged us to examine reactions of other α -phenylsulfonylphenones **2** promoted by **1a** and visible light irradiation to determine the effects of α -alkyl substitution and molecular oxygen concentration on reaction efficiencies and product distributions (Table 1). We observed that as the concentration of molecular oxygen increases ($\text{N}_2 < \text{air} < \text{O}_2$) in the atmosphere used for the visible light-induced reaction of **2a** and **1a**, the ratio of the oxidation product **4a** to reduction product **3a** increases (entries 1 and 2). On the other hand, **4a** is not produced when the reaction is carried out under a N₂ atmosphere (entry 3). It is interesting to note that the dark reaction of α -bromoisobutyrophenone with **1g** is significantly decelerated when a N₂ atmosphere is employed,²⁰ but the rate of the photoreaction of **2a** with **1a** under N₂ is not significantly decreased (compare entry 3 to entries 1 and 2). A similar trend is seen in the reaction of α -benzylphenone **2b** ($E_{1/2}^{\text{red}} = -1.48$ V vs SCE, see Table S1)^{19a} where oxidation product **4b** is not formed when a N₂ atmosphere is used

(entries 4, 5, and 6). Moreover, the reaction of acetophenone (α -non-alkylated phenone) **2c** ($E_{1/2}^{\text{red}} = -1.26$ V vs SCE, see Figure S3 and Table S1) does not produce oxidation product **4c** even when the reaction is carried out under an O_2 atmosphere (entries 7, 8, and 9). A final notable finding is that the more highly alkylated (sterically more crowded) **2a** produces **4a** in a higher relative ratio than the less alkylated (sterically less crowded) **2b** that forms **4b** (compare entries 1 and 2 to entries 4 and 5, respectively). This is similar to the trend observed earlier for reactions of the corresponding bromoketones with **1g**.²⁰

In order to explore the effect of light irradiation, the shorter time (20 min) reaction of **2a** with **1a** was carried out using LED or stirring in the dark (Table 2). As mentioned above, the

Table 2. Reactions of **2a** with **1a** in DMSO or MeCN under Air Upon Irradiation or in the Dark^a



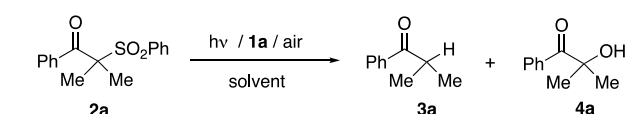
entry	irradiation or dark	solvent	conv of 2a (%) ^b	yields (%) ^b		ratio (%)	
				3a	4a	3	4
1	irradiation	DMSO	38	20	7	74	26
2	dark	DMSO	15	trace	8		
3	irradiation	MeCN	38	6	14	30	70
4	dark	MeCN	14	trace	trace		

^a**2a** (0.10 mmol), **1a** (1.2 equiv vs **2a**), solvent (1.0 mL), irradiated with 7.3 W white LED or stirred in the dark, 20 min. ^bDetermined by using ¹H NMR.

reaction of **2a** and **1a** in the dark takes place slowly to form **3a** and **4a** in significantly low yields (entries 2 and 4). On the other hand, **3a** and **4a** are formed in an ca. 7:3 ratio when a mixture of **2a** and **1a** in DMSO is irradiated, and the ratio is independent of the irradiation time (compare entry 1 with entry 2 of Table 1). Interestingly, the **3a** to **4a** ratio (3:7) for the photoreaction of **2a** and **1a** in MeCN is reverse of the process occurring in DMSO (entry 3). This finding encouraged us to examine the photoreactions of **2a** with **1a** in a variety of solvents having different polarities²⁵ and molecular oxygen solubilities.²⁶ The results given in Table 3 show that the ratios of the reduction to oxidation products (**3a** to **4a**) are governed by solvent utilization. Specifically, while hydroxyphenone **4a** is produced predominantly when polar alcohols and MeCN are used (entries 1–4), **3a** is the major product in reactions taking place in less polar DMSO, *N,N*-dimethylformamide (DMF), CH_2Cl_2 , tetrahydrofuran (THF), and PhCH_3 (entries 5–9). The **3a** to **4a** ratios differ significantly for reactions carried out in MeCN, DMSO and DMF, even though these solvents have quite similar polarities. Thus, the observed differences could be a consequence of oxygen concentration effects because the solubilities of O_2 in these solvents (DMSO < DMF < MeCN) parallel the **3a**:**4a** ratios (see entries 4, 5 and 6).

Photoreactions of α -arylsulfonylisobutyrophenones containing different para-substituents on both aryl rings **2d** ($E_{1/2}^{\text{red}} = -1.78$ V vs SCE), **2e** ($E_{1/2}^{\text{red}} = -1.64$ V vs SCE), **2f** ($E_{1/2}^{\text{red}} = -1.68$ V vs SCE), and **2g** ($E_{1/2}^{\text{red}} = -1.74$ V vs SCE) were also examined (Table 4, see Figure S3 and Table S1). Then, the reversed product ratios of **3** to **4** in the reactions between

Table 3. Photoreaction of **2a** with **1a** under Air in Different Solvents^a



entry	solvent	E_T ^b	[O_2] ^c	conv of 2a (%) ^d	yields (%) ^d		ratio (%)	
					3a	4a	3a	4a
1	MeOH	55.4	10.25	87	8	46	15	85
2	EtOH	51.9	10.0	87	11	42	21	79
3	<i>i</i> PrOH	48.4	10.24	94	15	57	21	79
4	MeCN	45.6	8.10	90	6	54	10	90
5 ^e	DMSO	45.1	2.21	100	65	23	74	26
6	DMF	43.2	5.05	100	40	29	58	42
7	CH_2Cl_2	40.7	11.08	92	45	34	57	43
8	THF	37.4	10.07	95	53	41	56	44
9	PhCH_3	33.9	8.72	86	38	24	61	39

^a**2a** (0.10 mmol), **1a** (1.2 equiv vs **2a**), solvent (1.0 mL), 7.3 W white LED, 4 h. ^bEmpirical parameter of solvent polarity (E_T (30), kcal/mol).²⁵ ^c O_2 solubility (mM) at 25 °C and 1 atm.^{26b} ^dDetermined by using ¹H NMR. ^eSame as entry 2 of Table 1.

DMSO and MeCN were again observed (compare entries 1–5 with entries 6–10). Apparently, the product ratios observed in both DMSO (entries 1–3) and MeCN (entries 6–8) are not greatly correlated with the electronic nature of the benzoyl substituents (*X*). On the other hand, although not significant, more electron-donating substituent (*Y*) of arylsulfonyl obviously increases the yield of **3** both in DMSO (entries 1, 4 and 5) and in MeCN (entries 6, 9 and 10). For example, the yield of **3a** from **2g** is greater than that from **2a** (compare entries 5 and 10 with entries 1 and 6, respectively). Consequently, the ratio of **3** to **4** increases in the order of **2a**, **2f**, and **2g**.

Since the generation of radical anions of **2** (**2^{•-}**) is expected in the reactions described above, density functional theory (DFT) calculations to gain information of the frontier orbital of **2a** and intermediacy of **2a^{•-}** were performed (Figure 3, also see Figure S4 and Table S2). As seen in Figure 3 (left), an antibonding interaction between α -carbon and sulfur atoms can be distinguished in the lowest unoccupied molecular orbital (LUMO) of **2a**. SET to **2a** produces **2a^{•-}** as a local energy minimum structure (center) which is derived from neutral **2a** as an initial geometry (see Figure S4 and Table S2). This initially formed radical anion is transformed to dissociated radical anion fragments as a global energy minimum structure shown in Figure 3 (right), which possesses significantly elongated carbon-sulfur bond from that of **2a**. Furthermore, a negative charge density is mostly populated on the sulfinate rather than on the α -keto alkyl fragment (Table S2). Therefore, **2a^{•-}** would undergo decomposition with a small activation energy to generate α -ketoalkyl radical and benzenesulfinate anion, which must be further assisted by α -dimethyl substitution (see Table S3, Figures S5 and S6). This behavior is contrastive to the radical anion of α -bromoisobutyrophenone in which dissociative electron transfer was previously proposed (also see Figure S5).²⁰ In principle, stabilization of the anionic leaving group assists α -carbon-heteroatom bond cleavage of radical anions of α -heterosubstituted arylketones.^{23d,g} Thus, in the reactions of α -

Table 4. Photoreactions of **2** with **1a** under Air^a

entry	2	X	Y	solvent	conv of 2 (%) ^b	yields (%) ^b		ratio (%)	
						3	4	3	4
1 ^c	2a	H	H	DMSO	100	65	23	74	26
2	2d	Me	H	DMSO	100	72	18	80	20
3	2e	Cl	H	DMSO	100	69	18	79	21
4	2f	H	Me	DMSO	100	70	15	82	18
5	2g	H	MeO	DMSO	100	72	12	86	14
6 ^d	2a	H	H	MeCN	90	6	54	10	90
7	2d	Me	H	MeCN	85	6	45	12	88
8	2e	Cl	H	MeCN	92	20	55	27	73
9	2f	H	Me	MeCN	78	7	56	11	89
10	2g	H	MeO	MeCN	79	11	50	18	82

^a2 (0.10 mmol), **1a** (1.2 equiv vs **2**), solvent (1.0 mL), 7.3 W white LED, 4 h. ^bDetermined by using ¹H NMR. ^cSame as entry 2 of Table 1. ^dSame as entry 4 of Table 3.

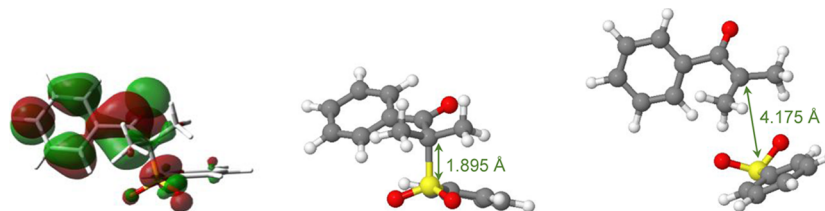
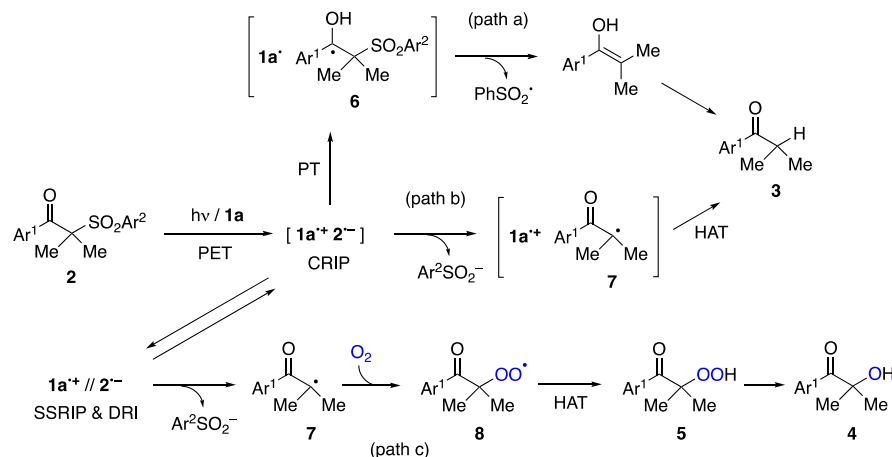


Figure 3. LUMO of **2a** (the isosurface value is set to 0.02) (left) and optimized structure of **2a**^{•-} (center) and dissociated radical anion fragments (right) are calculated at the ω B97X-D/6-31+G* level.

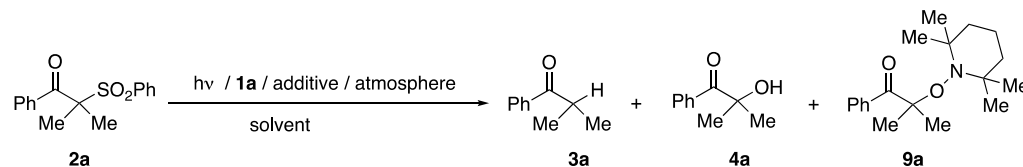
Scheme 2. Mechanistic Rationalization for the Solvent Dependence of the **3** to **4** Product Ratios in Photoreaction of **1a** and **2**



arylsulfonylisobutyrophenones **2** (see Table 4), the liberated arylsulfinate anion ($\text{YC}_6\text{H}_4\text{SO}_2^-$) is destabilized by an electron-donating substituent (Y) so that the fragmentation of radical anion of **2** should be decelerated in the order of **2a**, **2f**, and **2g**, which is also suggested by DFT calculations of reactivities of their radical anions (see Table S3 and Figure S6).

Following the suggestion arising from Fessenden's pioneering studies on the PET reaction of benzophenone and diethylaniline,^{21b} a plausible mechanistic pathway to rationalize the observations described above is outlined in Scheme 2. The route involves initial production of a CRIP formed by SET from photoexcited **1a** to **2** and comprised of radical cation of

1a (**1a**^{•+}) and radical anion of **2** (**2**^{•-}). It is anticipated that the CRIP would have a longer lifetime in less polar solvents. Moreover, PT from **1a**^{•+} to **2**^{•-} within the CRIP yields protonated ketyl **6**, which upon elimination of the phenylsulfinyl radical produces an enol as the precursor of the reduction product **3** (path a). Thus, if fragmentation of **2**^{•-} is decelerated, yield of **3** would increase, which was witnessed in the reactions of **2a**, **2f**, and **2g** (see above discussion for Table 4). Alternatively, loss of arylsulfinate from **2**^{•-} occurs in the CRIP to form a ketoalkyl radical **7**, which upon HAT from **1a**^{•+} would directly generate **3** (path b).²⁷ On the other hand, the CRIP should collapse to form a solvent separated radical ion pair or dissociated radical ions in more highly polar

Table 5. Photoreactions of 2a with 1a in the Presence of PhSH or TEMPO^a

entry	atmosphere	additive	solvent	irrad time (h)	conv of 2a (%) ^b	yields (%) ^b		
						3a	4a	9a
1 ^c	air		DMSO	4	100	65	23	
2	air	PhSH	DMSO	6	100	82	10	
3	air	TEMPO	DMSO	6	57	0	0	36
4	N ₂	TEMPO	DMSO	6	57	0	0	44
5	air	TEMPO	MeCN	6	40	0	0	26
6	N ₂	TEMPO	MeCN	6	37	0	0	34

^a2a (0.10 mmol), 1a (1.2 equiv vs 2a), additive: PhSH (3.0 equiv vs 2a), TEMPO (1.0 equiv vs 2a), solvent (1.0 mL), 7.3 W white LED.

^bDetermined by using ¹H NMR. ^cSame as entry 2 of Table 1.

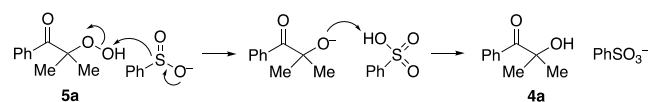
solvents. In both species, the oppositely charged radical ions are separated, and as a result, PT from 1a^{•+} to 2^{•-} and HAT from 1a^{•+} to 7 should take place more slowly. This circumstance would enable 2^{•-} to undergo loss of arylsulfinate to generate 7, which captures molecular oxygen to form hydroperoxy radical 8 as the precursor of the corresponding hydroperoxide 5 and the oxidation product 4 (path c). Furthermore, the proposed pathway is in accordance with the observed influence of molecular oxygen concentration on the product ratios.²⁶

As described above, α -ketoalkyl radical 7 is the likely intermediate in the pathway for the formation of 3 and 4 in the photoreaction of 1a with 2. To test this proposal, we designed experiments in which 7a generated from the reaction of 1a and 2a would be trapped by appropriate reagents such as thiophenol (PhSH) and 2,2,6,6-tetramethylpiperidine 1-oxyl (TEMPO) (Table 5). Visible light irradiation of a solution of 1a and 2a in air-saturated DMSO containing PhSH was found to promote the formation of a larger ratio of 3a to 4a than when PhSH is absent (compare entry 2 to entry 1). This result suggests that PhSH acts as a hydrogen atom donor to trap 7a. Second, irradiation of TEMPO containing DMSO or MeCN solution of 1a and 2a under an air or N₂ atmosphere leads to production of α -TEMPO adduct 9a, while 3a and 4a are not generated (entries 3–6). Thus, TEMPO trapping of 7a would be more efficient than O₂ trapping and HAT (from 1a^{•+}) of 7a. It is also worthy to note that the reaction is significantly retarded, which could be partly a result of the competitive consumption of 1a by TEMPO, although this reaction mechanism is not yet clarified.²⁸ In addition, irradiation of a solution of 2a (0.10 mmol) and TEMPO (0.10 mmol) in DMSO (1.0 mL) under N₂ with a 500 W Xe-lamp ($\lambda > 390$ nm) for 4 h leads to consumption of only a small quantity of 2a (6%) and not to formation of 9a (not shown in Table 5). This observation clearly suggests that 1a is essential to promote the reaction of 2a with TEMPO to produce 9a.

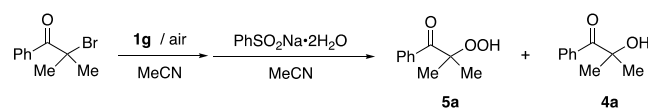
A question that remains unanswered is why α -hydroperoxy ketone 5a, an obvious precursor of α -hydroxyl ketone 4a (see Scheme 2), is not observed in the mixture of products arising from reactions of 2a with 1a. To gain insight into this question, we monitored the progress of the process by using ¹H NMR (Figures S7 and S8). The results show that 5a is indeed formed during the reaction, but it is subsequently converted to the corresponding hydroxyketone 4a in situ. In search for a

possible source of the reducing agent responsible for conversion of 5a to 4a, we became aware of the earlier observation showing that hydrogen peroxide is reduced during its reaction with sulfenic acid (RSOH) to form sulfonic acid (RSO₃H) via sulfinic acid (RSO₂H).²⁹ Thus, it is likely that the phenylsulfinate ion liberated from 2a^{•-} is the agent responsible for transforming 5a to 4a (Scheme 3). In order to assess this

Scheme 3. Hypothetical Reaction Pathways for Reduction of α -Hydroperoxy Ketone 5a by Sulfinate Anion to Produce α -Hydroxy Ketone 4a



hypothesis, we first prepared 5a by the reaction of α -bromoisobutyrophenone with 1g²⁰ and then treated it in the presence or absence of PhSO₂Na (Table 6). While 5a remains mostly unreacted when PhSO₂Na is absent (entry 1), most of the hydroperoxide is converted to 4a when PhSO₂Na is present (entry 2).

Table 6. Reduction of α -Hydroperoxyisobutyrophenone 5a by Benzenesulfinate^a

entry	PhSO ₂ Na·2H ₂ O	conv of bromoketone (%) ^b	yields (%) ^b	
			5a	4a
1	not added	100	55	7
2	added	100	7	56

^aBromoketone (0.10 mmol), 1g (1.5 equiv vs bromoketone), MeCN (2.0 mL), 1 h; PhSO₂Na·2H₂O (1.0 equiv vs bromoketone), 3 h.

^bDetermined by using ¹H NMR.

Based on previous considerations,^{18d} we propose that in the processes described above, 1a is ultimately converted to the oxidized form 10a through a pathway involving sequential electron, proton, and hydrogen atom transfer (Scheme 4). Formulation of a detailed stepwise route for this conversion is informed by the observation that photoexcitation enhances the

Scheme 4. Pathways for PET-Promoted Oxidation of 1a

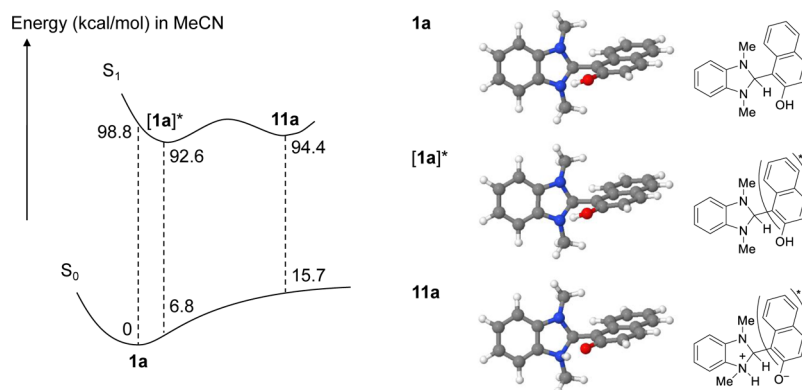
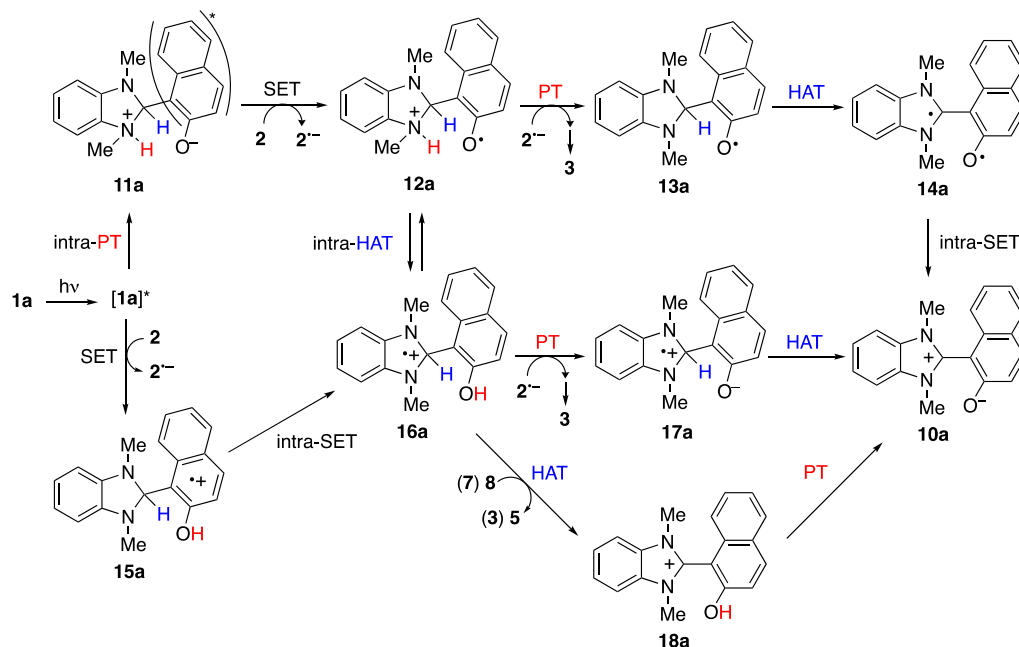
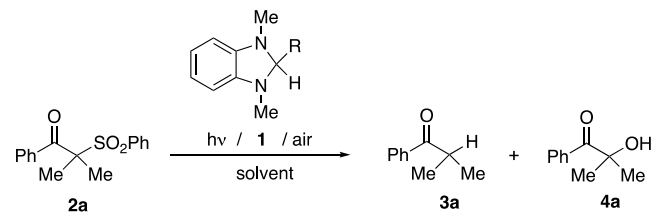


Figure 4. Optimized structures and diagram of the energies for the ground state **1a**, initial excited state **[1a]***, and excited naphthoxide **11a**. Energies and optimized structures are calculated by TD- ω B97X-D/6-31+G(d) level.

acidity of 2-naphthol toward deprotonation to produce the excited state of naphthoxide.³⁰ Moreover, the existence of intramolecular hydrogen-bonding between the hydroxyl of the naphthol moiety and benzimidazoline nitrogen in **1a** was previously demonstrated by using ¹H NMR spectroscopy (also see Table S4).^{18d} Thus, a suitable conformation enabling intramolecular PT (intra-PT) to occur between these moieties should exist in the initially formed excited state of **1a**. Consequently, we suggest that photoexcited **1a** (**[1a]***) undergoes intra-PT to form **11a** containing a protonated benzimidazoline group and an excited naphthoxide moiety. Subsequent SET from **11a** to **2** then produces the naphthoxy radical possessing a protonated imidazolyl **12a** (distonic radical cation) and **2^{•-}**. PT takes place to transform **12a** to **13a** with simultaneous production of **3** (see path a in Scheme 2), and HAT from **13a** followed by intramolecular SET (intra-SET) via **14a** produces betaine **10a**.³¹ Alternatively, if SET to **2** occurs from the naphthol moiety of **[1a]*** to form the naphthol radical cation **15a**, exergonic intra-SET from the benzimidazoline moiety to the naphthol radical cation should rapidly ensue owing its thermodynamic facility ($E_{1/2}^{\text{ox}}$ of BIH-Ar

and BIH-ArOH = +0.33 to +0.37 V vs SCE,^{18a,d} $E_{1/2}^{\text{ox}}$ of 1-methyl-2-naphthol = +1.32 V vs SCE^{18d}). This sequence produces benzimidazoline radical cation **16a**,^{18a} which undergoes PT from the naphthol moiety to yield **17a** accompanied by the formation of **3** (see path a in Scheme 2), and HAT from the benzimidazoline radical cation moiety to form **10a** occurs.³¹ However, if **16a** is cogenerated along with α -ketoalkyl radical **7** (see path b in Scheme 2) and hydroperoxy radical **8** (see path c in Scheme 2), HAT should precede PT and produce the stable imidazolium cation **18a** to afford **3** and **5**, respectively, while the former process is a minor one.³¹

DFT calculations were performed in order to gain information about the energies and structures of species involved in photoreactions of **1a** with **2** including **1a**, **[1a]***, **11a**, **12a**, and **16a**. The diagram of the calculated energies and optimized structures of **1a**, **[1a]*** (the initial excited state generated from **1a**), and the excited naphthoxide **11a** formed via subsequent intramolecular PT is given in Figure 4. The results suggest that **11a** is more stable in polar solvents than in the gas phase (see Table S5, Figures S11 and S12). Thus, **11a** is a plausible excited species for the solution-state reaction

Table 7. Photoreactions of 2a with Various Benzimidazolines 1 under Air^a


entry	1	R	solvent	conv of 2a (%) ^b	yields (%) ^b		ratio (%)	
					3a	4a	3a	4a
1 ^c	1a	1-(2-HO-naphthyl)	DMSO	100	65	23	74	26
2	1b	<i>o</i> -HOC ₆ H ₄	DMSO	91	37	49	43	57
3	1b	<i>o</i> -HOC ₆ H ₄	MeCN	77	trace	75	~0	~100
4	1c	<i>p</i> -HOC ₆ H ₄	DMSO	68	10	47	18	82
5	1d	3,5-Me-4-HOC ₆ H ₄	DMSO	80	8	51	14	86
6	1e	<i>m</i> -HOC ₆ H ₄	DMSO	58	7	44	14	86
7	1f	1-naphthyl	DMSO	50	11	36	23	77
8 ^d	1f	1-naphthyl	DMSO	60	19	31	38	62

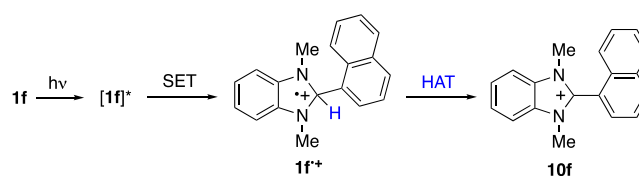
^a2a (0.10 mmol), 1 (1.2 equiv vs 2a), solvent (1.0 mL), 7.3 W white LED, 4 h. ^bDetermined by using ¹H NMR. ^cSame as entry 2 of Table 1. ^dAcOH (6.0 equiv vs 2a) was added.

system described in this study. Because [1a]^{*} as well as 11a are converted to 16a and 12a, respectively, through SET to 2 (also see Scheme 2), we next explored the reaction pathways followed by 12a and 16a by using DFT calculations. While the existence of an equilibrium between 12a and 16a through an intramolecular HAT (intra-HAT) is possible (Scheme 4), the DFT calculation results suggest that 12a is much less stable than 16a (see Tables S6, S7 and Figure S13). Thus, even if it were to form, 12a would rapidly rearrange to produce 16a.

If a PT process in the CRIP is involved in forming the reduction product in the photoreaction of α -phenylsulfonylphenone 2, the structure of the promoter BIH-ArOH or BIH-Ar is expected to influence the ratio of the reduction and oxidation products 3 to 4 produced. To explore this issue, photoreactions of 2a using variously substituted benzimidazolines 1 were performed (Table 7). The results show that when 1a is replaced by naphthylbenzimidazoline 1f, the 3a/4a ratio changes from 74:26 to 23:77 (compare entry 7 with entry 1). Moreover, addition of AcOH to the mixture of 1f and 2a causes a change in the 3a/4a ratio to 38:62 (entry 8). These observations are consistent with the proposal that PT to 2a^{*} occurs in the pathway for formation of 3a (see path a in Scheme 2). Notably, the 3a (14–43%) to 4a (86–57%) ratios observed for reactions promoted by hydroxyphenylbenzimidazolines 1b–1e in DMSO (entries 2, 4, 5, and 6) are the reverse of that in the reaction using 1a (entry 1) in the same solvent. Finally, when the solvent is changed from DMSO to MeCN for the reaction using *o*-hydroxyphenylbenzimidazoline 1b, 4a is exclusively produced (compare entry 3 to entry 2).

According to Zhu's pioneering work, thermodynamic considerations suggest that radical cations of 2-arylbenzimidazolines (BIH-Ar) should more readily undergo hydrogen atom donation than deprotonation from the C₂ position because the resulting cations are much more stable than the corresponding radicals.^{8b} However, as we previously discussed, deprotonation of the benzimidazoline radical cation could occur if the coproduced substrate radical anion is sufficiently basic.³² In any event, it is expected that the nonhydroxyaryl-substituted benzimidazoline 1f would be oxidized during its reaction with 2a by a sequence involving HAT as shown in Scheme 5. In

Scheme 5. Pathway for PET-Promoted Oxidation of 1f



addition, the radical anion of 2a is expected to undergo efficient fragmentation to form α -ketoalkyl radical 7a in a route that does not require an initial PT step. Moreover, HAT from the radical cation 1f^{•+} to the relatively bulky α -ketoalkyl radical 7a might be slower than the molecular oxygen trapping of 7a giving the peroxy radical 8a, which becomes 5a via HAT from 1f^{•+}. If an intra-PT occurs in the photoexcited state of *ortho*-hydroxyphenyl substituted benzimidazoline 1b in a manner similar to 1a (see Table S4 and Scheme 4), it must be less efficient than that for 1a.³³ On the other hand, intra-PT of other hydroxyphenyl substituted benzimidazolines 1c–1e from the phenol moieties to the distant benzimidazoline moieties is unlikely (also see Table S4). Thus, like 1f^{•+}, the radical cations of 1c–1e should preferably undergo sequential HAT and PT rather than a pathway involving initial PT followed by HAT (see similar pathways from 16a to 10a in Scheme 4). Indeed, the ratios of 3a to 4a generated from 2a in reactions promoted by 1c–1e are similar and close to that for 1f-induced processes (see entries 4, 5, 6, and 7 of Table 7). In contrast, 2a reacts with 1b to form 4a to 3a ratio that is less than those from reactions promoted by 1c–1e and more than that for 1a (see entries 1, 2, 4, 5, and 6 of Table 7).

CONCLUSIONS

PET is a fundamental process by which geminate radical ion pairs are formed from neutral electron donors and acceptors.² In organic solvents, dissociation of these radical ion pairs into separated radical ions is governed by the polarity of the medium.^{2a} In the investigation described above, we explored competitive visible light-induced reduction and oxidation reactions of α -phenylsulfonylphenones promoted by hydroxynaphthylbenzimidazolines (BIH-NapOH), in which product

ratios are governed by the contact versus solvent separated nature of radical ion intermediates. We found that photo-excited BIH-NapOH promotes reactions of sulfonylphenones under aerobic conditions that occur by competitive reduction (forming alkylphenones) and oxidation (producing α -hydroxyphenones) through pathways involving the intermediacies of ketone radical anions and α -ketoalkyl radicals. An assessment was made to determine how the ratios of reduction and oxidation products are influenced by several factors including molecular oxygen concentration, solvent polarity, nature of substituent on sulfonylketones, and structures of benzimidazole donors. The results suggest that oxidation products are produced by dissociation of α -ketoalkyl radicals from initially formed, solvent-caged radical ion pairs followed by reaction with molecular oxygen. In addition, the observations indicate that reduction products are generated by PT in solvent-caged benzimidazole and sulfonylphenone-derived radical ion pairs. Moreover, we proposed that arylsulfinate anions arising by carbon-sulfur bond cleavage of sulfonylketone radical anions act as reductants for oxidative conversion of initially formed α -hydroperoxyketones to α -hydroxyketones. Finally, DFT calculations were performed to explore the structures and properties of radical ions and other intermediates generated from BIH-NapOH as well as α -sulfonylketones. Although numerous examples of PET reactions of carbonyl substrates and amines have been reported, to the best of our knowledge, the current investigation focusing on competitive reduction and oxidation reactions taking place via radical intermediates derived from PET processes under the aerobic conditions is unique.²¹ In addition, because of the rising interest taking place in applications of BIH-Ar and BIH-ArOH,^{10–16} the observation of a solvent-dependent nature of their PET reactivities is important. Our continuing investigations of PET reactions utilizing BIH-Ar and BIH-ArOH as photoreductants^{17–19} are aimed at gaining a deeper understanding of reaction mechanisms and at developing mechanism-based protocols to control their PET reaction.

EXPERIMENTAL SECTION

General Methods. ¹H and ¹³C{¹H} NMR spectra were recorded on CDCl₃, DMSO-*d*₆, and CD₃CN with tetramethylsilane (Me₄Si) as an internal standard at 400 MHz for ¹H NMR and 100 MHz for ¹³C NMR. High-resolution mass spectra (HRMS) were recorded on an electrospray ionization (ESI) Orbitrap spectrometer. Uncorrected melting points were reported. Reduction potentials in MeCN were measured using cyclic voltammetry and a previously described procedure.³⁴ Conversion of the measured potentials (V vs Ag/AgNO₃) to the reported potentials (V vs SCE) was performed by using the formal potential of ferrocene/ferrocenium couple (0.439 V vs SCE) and the difference (0.373 V) of the potentials between Ag/AgNO₃ and SCE. Half-wave reduction potentials ($E_{1/2}^{\text{red}}$) reported in the manuscript were obtained from peak potentials by adding 0.029 V. The light source for photoreactions was a 7.3 W white LED (Toshiba bulb-type LED light: LDA7N-G-K). Column chromatography was performed with silica gel. Anhydrous solvents for reactions were obtained as follows. THF was distilled over sodium benzophenone under N₂. CH₂Cl₂ and PhCH₃ were purified in the same manner by the treatment with H₂SO₄, water, 5% NaOH, water, and CaCl₂ and then distilled over CaH₂. MeCN was distilled over P₂O₅ and subsequently distilled with K₂CO₃. Anhydrous DMF, DMSO, MeOH, EtOH, and *i*PrOH were purchased and used without distillation. Other reagents and solvents were used without further purification.

Preparation of Benzimidazolines. 1,3-Dimethylbenzimidazoline derivatives **1a**,^{18a} **1b**,³⁵ **1c**,³⁵ **1d**,^{19b} **1e**,^{19b} **1f**,^{18a} and **1g**^{9a} are

known compounds and were prepared using previously reported procedures.^{18a,35}

Preparation of Substrates. Sulfonylketones **2** were prepared by arylsulfination of the corresponding bromides. Preparations of **2d**, **2e**, and **2g** are described below. **2a**,³⁶ **2b**,³⁷ **2c**,³⁶ and **2f**³⁸ are known compounds.

Synthesis of 2-Phenylsulfonyl-2-methyl-1-(4-methylphenyl)-1-propanone (2d). A DMF (1.0 mL) solution containing 2-bromo-2-methyl-1-(4-methylphenyl)-1-propanone (121 mg, 0.50 mmol) and PhSO₂Na·2H₂O (201 mg, 1.0 mmol, 2.0 equiv) was purged with N₂ and then stirred at room temperature for 17 h. The mixture was diluted with water (30 mL) and extracted with EtOAc (20 mL × 3). The combined extracts were washed with water (30 mL × 2), sat. aq Na₂S₂O₃ (30 mL), and brine (30 mL), dried over anhydrous MgSO₄, and concentrated in vacuo to give a white solid. The solid was washed with water to give **2d** (114 mg, 0.38 mmol, 76%); mp 82.0–84.0 °C; ¹H NMR (400 MHz, DMSO-*d*₆): δ 7.82–7.74 (m, 5H), 7.66 (t, *J* = 7.8 Hz, 2H), 7.30 (d, *J* = 8.0 Hz, 2H), 2.37 (s, 3H), 1.60 (s, 6H). ¹³C{¹H} NMR (100 MHz, CDCl₃): 198.5, 143.2, 135.9, 135.4, 134.9, 134.3, 130.6, 129.5, 129.0, 73.6, 22.8, 21.7; HRMS (ESI) *m/z*: calcd for C₁₇H₁₈O₃S [M + H]⁺, 303.1049; found, 303.1044.

Synthesis of 2-Phenylsulfonyl-2-methyl-1-(4-chlorophenyl)-1-propanone (2e). A DMF (1.0 mL) solution containing 2-bromo-2-methyl-1-(4-chlorophenyl)-1-propanone (131 mg, 0.50 mmol) and PhSO₂Na·2H₂O (201 mg, 1.0 mmol, 2.0 equiv) was purged with N₂ and then stirred at room temperature for 15 h. The mixture was diluted with water (30 mL) and extracted with EtOAc (20 mL × 3). The combined extracts were washed with water (30 mL × 2), sat. aq Na₂S₂O₃ (30 mL), and brine (30 mL), dried over anhydrous MgSO₄, and concentrated in vacuo to give a white solid. The solid was washed with water to give **2e** (114 mg, 0.35 mmol, 70%); mp 124.0–126.0 °C; ¹H NMR (400 MHz, CDCl₃): δ 7.95 (d, *J* = 8.4 Hz, 2H), 7.77 (t, *J* = 7.6 Hz, 2H), 7.68 (t, *J* = 7.6 Hz, 1H), 7.54 (t, *J* = 7.2 Hz, 2H), 7.43 (d, *J* = 8.8 Hz, 2H), 1.69 (s, 6H). ¹³C{¹H} NMR (100 MHz, CDCl₃): 198.0, 138.9, 135.9, 135.1, 134.4, 130.8, 130.5, 128.9, 128.7, 73.5, 22.8; HRMS (ESI) *m/z*: calcd for C₁₆H₁₅O₃SCl [M + H]⁺, 323.0503; found, 323.0502.

Synthesis of 2-[(4-Methoxyphenyl)sulfonyl]isobutyrophenone (2g). A mixture of α -bromo isobutyrophenone (114 mg, 0.50 mmol) and sodium 4-methoxybenzenesulfinate (194 mg, 1.0 mmol, 2.0 equiv) in DMF (1.5 mL) was stirred at room temperature for 19 h. The mixture was diluted with water (30 mL) and extracted with EtOAc/hexane = 1/4 (20 mL × 3). The combined extracts were washed with sat. Na₂S₂O₃ aq (30 mL × 2) and brine (30 mL), dried over anhydrous MgSO₄, and concentrated in vacuo to give a colorless oil. The oil was distilled (0.1 mmHg, 170 °C) to yield **2g** (56 mg, 0.17 mmol, 34%). ¹H NMR (400 MHz, CDCl₃): δ 7.95 (d, *J* = 7.2 Hz, 2H), 7.71 (t, *J* = 8.8 Hz, 2H), 7.53 (t, *J* = 7.4 Hz, 1H), 7.44 (t, *J* = 7.6 Hz, 1H), 6.98 (d, *J* = 8.8 Hz, 2H), 3.38 (s, 3H), 1.69 (s, 6H). ¹³C{¹H} NMR (100 MHz, CDCl₃): 199.8, 164.3, 137.9, 132.7, 132.1, 129.0, 128.32, 126.5, 114.1, 73.4, 55.8, 22.8; HRMS (ESI) *m/z*: calcd for C₁₇H₁₈O₄S [M + H]⁺, 319.0999; found, 319.0995.

Photoreaction Procedure. A general procedure for reactions under air is described below (for Tables 1, 3, 4, and 7). A solution of **1** (0.12 mmol) and **2** (0.10 mmol) in a solvent (1.0 mL) in a Pyrex test tube (1.4 cm diameter) fitted with a drying tube containing CaCl₂ is irradiated with a 7.3 W white LED at room temperature (the distance between the test tube and the LED lamp is approximately 2.0 cm). In the photoreaction of **2** with **1** under O₂ (see entries 1, 4 and 7 in Table 1) or N₂ (see entries 3, 6 and 9 in Table 1), the solution is purged with O₂ or N₂ for 10 min and then irradiated. The photolysate is diluted with water (30 mL) and extracted with CH₂Cl₂ or EtOAc (20 mL × 3). The combined extract is washed with water (30 mL × 2) and brine (30 mL), dried over anhydrous MgSO₄, and concentrated in vacuo to give a residue. The conversion of **2** and the yield of products are determined using ¹H NMR analysis of the residue with triphenylmethane as an internal reference in CDCl₃. Ketones **3b**,³⁹ **3d**,⁴⁰ and **3e**⁴⁰ and hydroxyketones **4b**,⁴¹ **4d**,⁴² and **4e**⁴² are known compounds, while **3a**, **3c**, and **4a** are commercial materials. Ketone **3a** and hydroxyketone **4a** are produced from the

reactions of **2f** and **2g**. ^1H NMR charts of the reaction mixtures of selected experiments using **1a** and **2** are presented in the [Supporting Information](#).

Preparative Photoreaction of 2a with 1a. Irradiation of a solution of **1a** (34.8 mg, 0.12 mmol) and **2a** (28.8 mg, 0.10 mol) in DMSO (1.0 mL) was carried out using a 7.3 W white LED under the same conditions as that used for the analytical reaction (see entry 2 of [Table 1](#)). The reaction mixture obtained after the same work-up procedure described above was subjected to column chromatography using CH_2Cl_2 to give **3a** (8.4 mg, 0.0568 mmol, 57%) and **4a** (3.9 mg, 0.0238 mmol, 24%). **3a**: colorless oil; ^1H NMR (400 MHz, CDCl_3): δ 7.96 (d, $J = 8.4$ Hz, 2H), 7.56 (t, $J = 7.4$ Hz, 1H), 7.47 (t, $J = 7.4$ Hz, 2H), 3.57 (sep, $J = 6.8$ Hz, 1H), 1.22 (d, 6H). **4a**: colorless oil; ^1H NMR (400 MHz, CDCl_3): δ 8.01 (d, $J = 8.4$ Hz, 2H), 7.58 (t, $J = 7.4$ Hz, 1H), 7.48 (t, $J = 7.6$ Hz, 2H), 4.08 (s, 1H), 1.64 (s, 6H). ^1H NMR charts of **3a** and **4a** obtained as above are shown in the [Supporting Information](#).

Reactions of 2a with 1a under Air upon Irradiation or in the Dark. A DMSO or MeCN (1.0 mL) solution containing **1a** (34.8 mg, 0.12 mmol) and **2a** (28.8 mg, 0.10 mol) was irradiated with a 7.3 W white LED at room temperature for 20 min (see entries 1 and 3 in [Table 2](#)). Alternatively, the same solution was stirred for 20 min at room temperature in the dark (see entries 2 and 4 in [Table 2](#)). Then, 2'-bromoacetophenone (0.12 mmol) was added to the mixture, and the resulting mixture was stirred for 10 min. After performing CH_2Cl_2 extraction, the crude product mixture obtained was subjected to ^1H NMR analysis to determine the yields of recovered **2a**, **3a**, and **4a**.

Photoreaction of 2a with 1a in the Presence of PhSH under Air. A DMSO (1.0 mL) solution containing **1a** (34.8 mg, 0.12 mmol), **2a** (28.8 mg, 0.10 mmol), and PhSH (32.0 μl , 0.30 mmol) was irradiated with a 7.3 W white LED at room temperature for 6 h. After performing CH_2Cl_2 extraction, the crude product mixture obtained was subjected to ^1H NMR analysis to determine the yields of recovered **2a**, **3a**, and **4a** (see entry 2 in [Table 5](#)).

Photoreaction of 2a with 1a in the Presence of TEMPO under Air or N_2 . An appropriate solvent (1.0 mL) containing **1a** (34.8 mg, 0.12 mmol), **2a** (28.8 mg, 0.10 mmol), and TEMPO (15.6 mg, 0.10 mmol) was irradiated with a 7.3 W white LED at room temperature for 6 h (see entries 3 and 5 in [Table 5](#)). In the photoreaction of **1a** and **2a** in the presence of TEMPO under N_2 , the solution is purged with N_2 for 10 min and then irradiated (see entries 4 and 6 in [Table 5](#)). After performing CH_2Cl_2 extraction, the crude product mixture obtained was analyzed by ^1H NMR to determine the conversion of **2a** and the formation of **9a**.⁴³ ^1H NMR chart of the reaction mixture is presented in the [Supporting Information](#).

Time Course for the Photoreaction of 2a and 1a in CD_3CN under Air Analyzed by ^1H NMR. To a mixture of **1a** (8.8 mg, 0.030 mmol) and **2a** (7.2 mg, 0.025 mmol) in a predried NMR testtube was added CD_3CN (0.40 mL). Then, the ^1H NMR spectrum of a resulting solution was measured (0 h). After the solution was irradiated with a 7.3 W white LED for 0.5, 1.0, and 2.0 h, the reaction at each time interval was analyzed by ^1H NMR. The results are reported in [Figure S7](#). Also ^1H NMR spectra of **4a**, **5a**, and their mixture are presented in [Figure S8](#).

Reduction of α -Hydroperoxyketone 5a by Benzenesulfinate. Following the reported procedure,²⁰ MeCN (2.0 mL) solution containing **1g** (33.6 mg, 0.15 mmol) and α -bromoisobutyrophenone (22.8 mg, 0.10 mmol) was stirred for 1 h at room temperature. Then, $\text{PhSO}_2\text{Na}\cdot 2\text{H}_2\text{O}$ (20.4 mg, 0.10 mmol) was added, and the resulting mixture was stirred for 3 h (see entry 2 in [Table 6](#)). As a control experiment, the solution was continuously stirred for additional 3 h without addition of $\text{PhSO}_2\text{Na}\cdot 2\text{H}_2\text{O}$ (see entry 1 in [Table 6](#)). After performing CH_2Cl_2 extraction, the crude product mixture obtained was subjected to ^1H NMR analysis to determine the yields of **5a**^{20,44} and **4a**.

DFT Calculations. Calculations were carried out using the Gaussian 16 program package.⁴⁵ The structures of closed shell species **1a** and **2a** were optimized at the restricted $\omega\text{B97X-D/6-31+G(d)}$ level, the functional of which includes long-range corrections and empirical dispersion,⁴⁶ while the structures of open

shell species **2a**^{*}, **12a**, and **16a** were optimized using the unrestricted theory at the same level. The structures of excited state (S_1) of **1a** and **11a** were optimized using time-dependent DFT theory. Frequency analysis was performed for each optimized structure to confirm that no or one imaginary frequency was obtained for the energy-minimum or the transition-state structures, respectively. These calculations were performed in gas phase or solution using the polarizable continuum model. To estimate the charge and spin distributions, natural population analysis built in the Gaussian was performed.⁴⁷ The optimized structure and molecular orbitals were visualized with GaussView 6.0⁴⁸ and Jmol.⁴⁹

■ ASSOCIATED CONTENT

Supporting Information

The Supporting Information is available free of charge at <https://pubs.acs.org/doi/10.1021/acs.joc.0c02666>.

Data of absorption spectra of **1**, cyclic voltammograms of **2**, ^1H NMR analysis of time course as well as deuterium labeling experiment for photoreaction of **1a** and **2a**, DFT calculations of **1**, **2**, and derived transient species, ^1H NMR charts of selected photoreaction products, and ^1H NMR, ^{13}C NMR spectra and HRMS data of deuterated **1a-d** and new **2** ([PDF](#))

■ AUTHOR INFORMATION

Corresponding Author

Eietsu Hasegawa – Department of Chemistry, Faculty of Science, Niigata University, Nishi-ku, Niigata 950-2181, Japan; orcid.org/0000-0002-4328-0917; Email: ehase@chem.sc.niigata-u.ac.jp

Authors

Shyota Nakamura – Department of Chemistry, Faculty of Science, Niigata University, Nishi-ku, Niigata 950-2181, Japan

Kazuki Oomori – Department of Chemistry, Faculty of Science, Niigata University, Nishi-ku, Niigata 950-2181, Japan

Tsukasa Tanaka – Department of Chemistry, Faculty of Science, Niigata University, Nishi-ku, Niigata 950-2181, Japan

Hajime Iwamoto – Department of Chemistry, Faculty of Science, Niigata University, Nishi-ku, Niigata 950-2181, Japan; orcid.org/0000-0001-7064-829X

Kan Wakamatsu – Department of Chemistry, Faculty of Science, Okayama University of Science, Kita-ku, Okayama 700-0005, Japan; orcid.org/0000-0002-7467-1005

Complete contact information is available at:

<https://pubs.acs.org/doi/10.1021/acs.joc.0c02666>

Notes

The authors declare no competing financial interest.

■ ACKNOWLEDGMENTS

This article is dedicated to the memories of Dr. Toshio Mukai (1924–2020) and Dr. Tsutomu Miyashi (1940–2020), both of whom are Professors Emeritus of Tohoku University and were graduate mentors of E.H. and K.W. This study was partly supported by JSPS KAKENHI grants (JP 19K05435 for E.H.).

■ REFERENCES

(1) Representative book chapters and reviews for electron transfer reactions. (a) Ebersson, L. *Electron Transfer Reactions in Organic*

Chemistry; Springer: Berlin, 1987. (b) *Advances in Electron Transfer Chemistry*; Mariano, P. S., Ed.; JAI Press: Greenwich, 1991–1999; Vol. 1–6. (c) Connelly, N. G.; Geiger, W. E. Chemical Redox Agents for Organometallic Chemistry. *Chem. Rev.* **1996**, *96*, 877–910. (d) *Electron Transfer in Chemistry*; Balzani, V., Ed.; Wiley-VCH: Weinheim, 2001; Vol. 1–5. (e) *Organic Electrochemistry*, 4th edn.; Lund, H., Hammerich, O., Eds.; Marcel Dekker: New York, 2001. (f) Todres, Z. V. *Ion-Radical Organic Chemistry Principles and Applications*, 2nd edn.; CRC Press: Boca Raton, 2009. (g) Zhang, N.; Samanta, S. R.; Rosen, B. M.; Percec, V. Single Electron Transfer in Radical Ion and Radical-Mediated Organic, Materials and Polymer Synthesis. *Chem. Rev.* **2014**, *114*, 5848–5958.

(2) Representative book chapters and reviews for photoinduced electron transfer. (a) Weller, A. Photoinduced Electron Transfer in Solution: Exciplex and Radical Ion Pair Formation Free Enthalpies and their Solvent Dependence. *Z. Phys. Chem.* **1982**, *133*, 93–98. (b) *Photoinduced Electron Transfer*; Fox, M. A., Chanon, M., Eds.; Elsevier: Amsterdam, 1988; Parts A–D. (c) Kavarnos, G. J. *Fundamental of Photoinduced Electron Transfer*; VCH Publishers: New York, 1993. (d) *CRC Handbook of Organic Photochemistry and Photobiology*, 1st ed.; Horspool, W. M., Song, P. S., Eds.; CRC Press: Boca Raton, FL, 1994; and 2nd ed.; Horspool, W. M., Lenci, F., Eds.; CRC Press: Boca Raton, FL, 2003. (e) Hoffmann, N. Efficient Photochemical Electron Transfer Sensitization of Homogeneous Organic Reactions. *J. Photochem. Photobiol., C* **2008**, *9*, 43–60.

(3) Pioneering works of synthetic application of photoredox catalysts. (a) Nicewicz, D. A.; MacMillan, D. W. C. Merging Photoredox Catalysis with Organocatalysis: The Direct Asymmetric Alkylation of Aldehydes. *Science* **2008**, *322*, 77–80. (b) Ischay, M. A.; Anzovino, M. E.; Du, J.; Yoon, T. P. Efficient Visible Light Photocatalysis of [2+2] Enone Cycloadditions. *J. Am. Chem. Soc.* **2008**, *130*, 12886–12887. (c) Narayanan, J. M. R.; Tucker, J. W.; Stephenson, C. R. J. Electron-Transfer Photoredox Catalysis: Development of a Tin-Free Reductive Dehalogenation Reaction. *J. Am. Chem. Soc.* **2009**, *131*, 8756–8757.

(4) Representative reviews of photoredox catalysts. (a) Narayanan, J. M. R.; Stephenson, C. R. J. Visible light photoredox catalysis: applications in organic synthesis. *Chem. Soc. Rev.* **2011**, *40*, 102–113. (b) Ravelli, D.; Fagnoni, M.; Albini, A. Photoorganocatalysis. What for? *Chem. Soc. Rev.* **2013**, *42*, 97–113. (c) Prier, C. K.; Rankic, D. A.; MacMillan, D. W. C. Visible Light Photoredox Catalysis with Transition Metal Complexes: Applications in Organic Synthesis. *Chem. Rev.* **2013**, *113*, 5322–5363. (d) Fukuzumi, S.; Ohkubo, K. Organic Synthetic Transformations using Organic Dyes as Photoredox Catalysts. *Org. Biomol. Chem.* **2014**, *12*, 6059–6071. (e) Hari, D. P.; König, B. Synthetic applications of eosin Y in photoredox catalysis. *Chem. Commun.* **2014**, *50*, 6688–6699. (f) Skubi, K. L.; Blum, T. R.; Yoon, T. P. Dual Catalysis Strategies in Photochemical Synthesis. *Chem. Rev.* **2016**, *116*, 10035–10074. (g) Romero, N. A.; Nicewicz, D. A. Organic Photoredox Catalysis. *Chem. Rev.* **2016**, *116*, 10075–10166. (h) Bogdos, M. K.; Pinard, E.; Murphy, J. A. Applications of Organocatalysed Visible-light Photoredox Reactions for Medicinal Chemistry. *Beilstein J. Org. Chem.* **2018**, *14*, 2035–2064. (i) Marzo, L.; Pagire, S. K.; Reiser, O.; König, B. Visible-Light Photocatalysis: Does It Make a Difference in Organic Synthesis? *Angew. Chem., Int. Ed.* **2018**, *57*, 10034–10072. (j) Buzzetti, L.; Crisenza, G. E. M.; Melchiorre, P. Mechanistic Studies in Photocatalysis. *Angew. Chem., Int. Ed.* **2019**, *58*, 3730–3747.

(5) (a) Cheng, X.; Wenhao, H. Hantzsch Esters as Multifunctional Reagents in Visible-Light Photoredox Catalysis. *Synlett* **2017**, *28*, 148–158. (b) Wang, P.-Z.; Chen, J.-R.; Xiao, W.-J. Hantzsch Esters: An Emerging Versatile Class of Reagents in Photoredox Catalyzed Organic Synthesis. *Org. Biomol. Chem.* **2019**, *17*, 6936–6951.

(6) Synthetic application of photoexcited Hantzsch esters. (a) Zhu, X.-Q.; Liu, Y.-C.; Cheng, J.-P. Which Hydrogen Atom Is First Transferred in the NAD(P)H Model Hantzsch Ester Mediated Reactions via One-Step and Multistep Hydride Transfer? *J. Org. Chem.* **1999**, *64*, 8980–8981. (b) Zhang, J.; Jin, M.-Z.; Zhang, W.; Yang, L.; Liu, Z.-L. Photoinduced Transformation of α,β -Epoxyke-

tones to β -Hydroxyketones by Hantzsch 1,4-Dihydropyridine. *Tetrahedron Lett.* **2002**, *43*, 9687–9689. (c) Jung, J.; Kim, J.; Park, G.; You, Y.; Cho, E. J. Selective Debromination and α -Hydroxylation of α -Bromo Ketones Using Hantzsch Esters as Photoreductants. *Adv. Synth. Catal.* **2016**, *358*, 74–80. (d) Chen, W.; Tao, H.; Huang, W.; Wang, G.; Li, S.; Cheng, X.; Li, G. Hantzsch Ester as a Photosensitizer for the Visible-Light-Induced Debromination of Vicinal Dibromo Compounds. *Chem.—Eur. J.* **2016**, *22*, 9546–9550. (e) Huang, X.; Luo, S.; Burghaus, O.; Webster, R. D.; Harms, K.; Meggers, E. Combining the Catalytic Enantioselective Reaction of Visible-Light-Generated Radicals with a Byproduct Utilization System. *Chem. Sci.* **2017**, *8*, 7126–7131. (f) Chen, D.; Xu, L.; Long, T.; Zhu, S.; Yang, J.; Chu, L. Metal-Free, Intermolecular Carbopyridylation of Alkenes via Visible-Light-Induced Reductive Radical Coupling. *Chem. Sci.* **2018**, *9*, 9012–9017. (g) Ji, P.; Zhang, Y.; Wei, Y.; Huang, H.; Hu, W.; Mariano, P. A.; Wang, W. Visible-Light-Mediated, Chemo- and Stereoselective Radical Process for the Synthesis of C-Glycoamino Acids. *Org. Lett.* **2019**, *21*, 3086–3092. (h) Wu, J.; Grant, P. S.; Li, X.; Noble, A.; Aggarwal, V. K. Catalyst-Free Deaminative Functionalizations of Primary Amines by Photoinduced Single-Electron Transfer. *Angew. Chem., Int. Ed.* **2019**, *58*, 5697–5701. (i) Konev, M. O.; Cardinale, L.; von Wangelin, A. J. Catalyst-Free N-Deoxygenation by Photoexcitation of Hantzsch Ester. *Org. Lett.* **2020**, *22*, 1316–1320. (j) Zhu, D. L.; Wu, Q.; Li, H. Y.; Li, H. X.; Lang, J. P. Hantzsch Ester as a Visible-Light Photoredox Catalyst for Transition-Metal-Free Coupling of Arylhalides and Arylsulfonates. *Chem.—Eur. J.* **2020**, *26*, 3484–3488.

(7) Various photoexcited organic reductants. (a) Fukuzumi, S.; Inada, O.; Suenobu, T. Mechanisms of Electron-Transfer Oxidation of NADH Analogues and Chemiluminescence. Detection of the Keto and Enol Radical Cations. *J. Am. Chem. Soc.* **2003**, *125*, 4808–4816. (b) Doni, E.; Mondal, B.; O'Sullivan, S.; Tuttle, T.; Murphy, J. A. Overturning Established Chemoselectivities: Selective Reduction of Arenes over Malonates and Cyanoacetates by Photoactivated Organic Electron Donors. *J. Am. Chem. Soc.* **2013**, *135*, 10934–10937. (c) Doni, E.; Murphy, J. A. Reductive Decyanation of Malononitriles and Cyanoacetates using Photoactivated Neutral Organic Super-electron-donors. *Org. Chem. Front.* **2014**, *1*, 1072–1076. (d) O'Sullivan, S.; Doni, E.; Tuttle, T.; Murphy, J. A. Metal-Free Reductive Cleavage of C–N and S–N Bonds by Photoactivated Electron Transfer from a Neutral Organic Donor. *Angew. Chem., Int. Ed.* **2014**, *53*, 474–478. (e) Xu, Z.; Gao, L.; Wang, L.; Gong, M.; Wang, W.; Yuan, R. Visible Light Photoredox Catalyzed Biaryl Synthesis Using Nitrogen Heterocycles as Promoter. *ACS Catal.* **2015**, *5*, 45–50. (f) Budén, M. E.; Bardagi, J. I.; Puiatti, M.; Rossi, R. A. Initiation in Photoredox C–H Functionalization Reactions. Is Dimsyl Anion a Key Ingredient? *J. Org. Chem.* **2017**, *82*, 8325–8333. (g) Nocera, G.; Young, A.; Palumbo, F.; Emery, K. J.; Coulthard, G.; McGuire, T.; Tuttle, T.; Murphy, J. A. Electron Transfer Reactions: KOTBu (but not NaOtBu) Photoreduces Benzophenone under Activation by Visible Light. *J. Am. Chem. Soc.* **2018**, *140*, 9751–9757. (h) Glaser, F.; Larsen, C. B.; Kerzig, C.; Wenger, O. S. Aryl Dechlorination and Defluorination with an Organic Super-Photoreductant. *Photochem. Photobiol. Sci.* **2020**, *19*, 1035–1041.

(8) (a) Lee, I.-S. H.; Jeoung, E. H.; Kreevoy, M. M. Marcus Theory of a Parallel Effect on a for Hydride Transfer Reaction between NAD⁺ Analogues. *J. Am. Chem. Soc.* **1997**, *119*, 2722–2728. (b) Zhu, X.-Q.; Zhang, M.-T.; Yu, A.; Wang, C.-H.; Cheng, J.-P. Hydride, Hydrogen Atom, Proton, and Electron Transfer Driving Forces of Various Five-Membered Heterocyclic Organic Hydrides and Their Reaction Intermediates in Acetonitrile. *J. Am. Chem. Soc.* **2008**, *130*, 2501–2516. (c) Horn, M.; Schappele, L. H.; Lang-Wittkowski, G.; Mayr, H.; Ofial, A. R. Towards a Comprehensive Hydride Donor Ability Scale. *Chem.—Eur. J.* **2013**, *19*, 249–263. (d) Ilic, S.; Pandey Kadel, U.; Basdogan, Y.; Keith, J. A.; Glusac, K. D. Thermodynamic Hydricities of Biomimetic Organic Hydride Donors. *J. Am. Chem. Soc.* **2018**, *140*, 4569–4579. (e) Ma, L.; Sakhaee, N.; Jafari, S.; Wilhelm, S.; Rahmani, P.; Lu, Y. Imbalanced Transition States from α -H/D and Remote β -Type N-CH/D Secondary Kinetic Isotope Effects on the NADH/

NAD⁺ Analogues in Their Hydride Tunneling Reactions in Solution. *J. Org. Chem.* **2019**, *84*, 5431–5439.

(9) Pioneering works of BIH-Ar redox chemistry. (a) Chikashita, H.; Itoh, K. AlCl₃-Promoted Conjugate Reduction of α,β -Unsaturated Carbonyl Compounds with 1,3-Dimethyl-2-phenylbenzimidazoline. *Bull. Chem. Soc. Jpn.* **1986**, *59*, 1747–1752. (b) Chikashita, H.; Ide, H.; Itoh, K. 1,3-Dimethyl-2-phenylbenzimidazoline as a Novel and Efficient Reagent for Mild Reductive Dehalogenation of α -Halo Carbonyl Compounds and Acid Chlorides. *J. Org. Chem.* **1986**, *51*, 5400–5405. (c) Chen, J.; Tanner, D. D. New Method for the Facile Reduction of α -Nitro Sulfones to Nitroalkanes via an Electron-Transfer-Hydrogen Atom Abstraction Mechanism. *J. Org. Chem.* **1988**, *53*, 3897–3900. (d) Tanner, D. D.; Chen, J. J. On the Mechanism of the Reduction of α -Haloketones by 1,3-Dimethyl-2-phenylbenzimidazoline. Reduction by a SET (single electron transfer)-Hydrogen Atom Abstraction Chain Mechanism. *J. Org. Chem.* **1989**, *54*, 3842–3846. (e) Tanner, D. D.; Chen, J. J.; Chen, L.; Luelo, C. Fragmentation of Substituted Acetophenones and Halobenzophenone Ketyls. Calibration of a Mechanistic Probe. *J. Am. Chem. Soc.* **1991**, *113*, 8074–8081.

(10) PET reactions. (a) Liu, Z.-L.; Yu, W.; Liu, Q.; Liu, Z.; Zhou, Y.-L.; Zhang, W.; Yang, L. Photochemical Desulfonation of *N*-Tosyl Amides by 2-Phenyl-*N,N'*-Dimethylbenzimidazoline (PDMBI). *Synlett* **2005**, 2510–2512. (b) Feng, Y.-S.; Yang, C.-Y.; Huang, Q.; Xu, H.-J. Study on Comparison of Reducing Ability of Three Organic Hydride Compounds. *Tetrahedron* **2012**, *68*, 5053–5059. (c) Zhang, Y.; Petersen, J. L.; Millsman, C. A Luminescent Zirconium(IV) Complex as a Molecular Photosensitizer for Visible Light Photoredox Catalysis. *J. Am. Chem. Soc.* **2016**, *138*, 13115–13118.

(11) Super electron donors. Rohrbach, S.; Shah, R. S.; Tuttle, T.; Murphy, J. A. Neutral Organic Super Electron Donors Made Catalytic. *Angew. Chem., Int. Ed.* **2019**, *58*, 11454–11458.

(12) Hydrogen gas evolution. (a) Brunet, P.; Wuest, J. D. Formal Transfer of Hydride from Carbon–Hydrogen Bonds. Attempted Generation of H₂ by Intramolecular Protonolyses of the Activated Carbon–Hydrogen Bonds of Dihydrobenzimidazoles. *Can. J. Chem.* **1996**, *74*, 689–696. (b) Schwarz, D. E.; Cameron, T. M.; Hay, P. J.; Scott, B. L.; Tumas, W.; Thorn, D. L. Hydrogen Evolution from Organic “Hydrides”. *Chem. Commun.* **2005**, 5919–5921.

(13) CO₂ reduction. (a) Tamaki, Y.; Koike, K.; Morimoto, T.; Ishitani, O. Substantial Improvement in the Efficiency and Durability of a Photocatalyst for Carbon Dioxide Reduction Using a Benzimidazole Derivative as an Electron Donor. *J. Catal.* **2013**, *304*, 22–28. (b) Tamaki, Y.; Ishitani, O. Supramolecular Photocatalysts for the Reduction of CO₂. *ACS Catal.* **2017**, *7*, 3394–3409. (c) Rao, H.; Bonin, J.; Robert, M. Non-Sensitized Selective Photochemical Reduction of CO₂ to CO under Visible Light with an Iron Molecular Catalyst. *Chem. Commun.* **2017**, *53*, 2830–2833. (d) Hong, D.; Tsukakoshi, Y.; Kotani, H.; Ishizuka, T.; Kojima, T. Visible-Light-Driven Photocatalytic CO₂ Reduction by a Ni(II) Complex Bearing a Bioinspired Tetradentate Ligand for Selective CO Production. *J. Am. Chem. Soc.* **2017**, *139*, 6538–6541. (e) Cheong, H.-Y.; Kim, S.-Y.; Cho, Y.-J.; Cho, D. W.; Kim, C. H.; Son, H.-J.; Pac, C.; Kang, S. O. Photosensitization Behavior of Ir(III) Complexes in Selective Reduction of CO₂ by Re(I)-Complex-Anchored TiO₂ Hybrid Catalyst. *Inorg. Chem.* **2017**, *56*, 12042–12053. (f) Lim, C.-H.; Ilic, S.; Alherz, A.; Worrell, B. T.; Bacon, S. S.; Hynes, J. T.; Glusac, K. D.; Musgrave, C. B. Benzimidazoles as Metal-Free and Recyclable Hydrides for CO₂ Reduction to Formate. *J. Am. Chem. Soc.* **2019**, *141*, 272–280.

(14) Solar cells. (a) Cho, N.; Yip, H.-L.; Davies, J. A.; Kazarinoff, P. D.; Zeigler, D. F.; Durban, M. M.; Segawa, Y.; O'Malley, K. M.; Luscombe, C. K.; Jen, A. K.-Y. In-situ Crosslinking and n-Doping of Semiconducting Polymers and their Application as Efficient Electron-Transporting Materials in Inverted Polymer Solar Cells. *Adv. Energy Mater.* **2011**, *1*, 1148–1153. (b) Kim, S. S.; Bae, S.; Jo, W. H. Performance Enhancement of Planar Heterojunction Perovskite Solar Cells by n-Doping of the Electron Transporting Layer. *Chem. Commun.* **2015**, *51*, 17413–17416.

(15) Organic semiconductors. (a) Wei, P.; Oh, J. H.; Dong, G.; Bao, Z. Use of a 1*H*-Benzimidazole Derivative as an *n*-Type Dopant and to Enable Air-Stable Solution-Processed *n*-Channel Organic Thin-Film Transistors. *J. Am. Chem. Soc.* **2010**, *132*, 8852–8853. (b) Naab, B. D.; Guo, S.; Olthof, S.; Evans, E. G. B.; Wei, P.; Millhauser, G. L.; Kahn, A.; Barlow, S.; Marder, S. R.; Bao, Z. Mechanistic Study on the Solution-Phase *n*-Doping of 1,3-Dimethyl-2-aryl-2,3-dihydro-1*H*-benzimidazole Derivatives. *J. Am. Chem. Soc.* **2013**, *135*, 15018–15025. (c) Schlitz, R. A.; Brunetti, F. G.; Glauddell, A. M.; Miller, P. L.; Brady, M. A.; Takacs, C. J.; Hawker, C. J.; Chabiny, M. L. Solubility-Limited Extrinsic *n*-Type Doping of a High Electron Mobility Polymer for Thermoelectric Applications. *Adv. Mater.* **2014**, *26*, 2825–2830. (d) Naab, B. D.; Zhang, S.; Vandewal, K.; Salleo, A.; Barlow, S.; Marder, S. R.; Bao, Z. Effective Solution- and Vacuum-Processed *n*-Doping by Dimers of Benzimidazole Radicals. *Adv. Mater.* **2014**, *26*, 4268–4272. (e) Schwarze, M.; Naab, B. D.; Tietze, M. L.; Scholz, R.; Pahner, P.; Bussoletti, F.; Kera, S.; Kasemann, D.; Bao, Z.; Leo, K. Analyzing the *n*-Doping Mechanism of an Air-Stable Small-Molecule Precursor. *ACS Appl. Mater. Interfaces* **2018**, *10*, 1340–1346.

(16) SO₂ conversion. Mehrotra, S.; Raj, S.; Jain, A. K.; Angamuthu, R. Benzimidazolines Convert Sulfur Dioxide to Bisulfate at Room Temperature and Atmospheric Pressure Utilizing Aerial Oxygen. *ACS Sustainable Chem. Eng.* **2017**, *5*, 6322–6328.

(17) Hasegawa, E.; Takizawa, S.-y. 2-Aryl-1,3-dimethylbenzimidazolines as Effective Electron and Hydrogen Donors in Photoinduced Electron-Transfer Reactions. *Aust. J. Chem.* **2015**, *68*, 1640–1647. . and references cited therein

(18) Photoexcited BIH-Ar and BIH-ArOH. (a) Hasegawa, E.; Ohta, T.; Tsuji, S.; Mori, K.; Uchida, K.; Miura, T.; Ikoma, T.; Tayama, E.; Iwamoto, H.; Takizawa, S.-y.; Murata, S. Aryl-Substituted Dimethylbenzimidazolines as Effective Reductants of Photoinduced Electron Transfer Reactions. *Tetrahedron* **2015**, *71*, 5494–5505. (b) Hasegawa, E.; Mori, K.; Tsuji, S.; Nemoto, K.; Ohta, T.; Iwamoto, H. Visible Light-Promoted Metal-Free Reduction of Organohalides by 2-Naphthyl or 2-Hydroxynaphthyl-Substituted 1,3-Dimethylbenzimidazolines. *Aust. J. Chem.* **2015**, *68*, 1648–1652. (c) Hasegawa, E.; Izumiya, N.; Fukuda, T.; Nemoto, K.; Iwamoto, H.; Takizawa, S.-y.; Murata, S. Visible Light-Promoted Reductive Transformations of Various Organic Substances by Using Hydroxyaryl-Substituted Benzimidazolines and Bases. *Tetrahedron* **2016**, *72*, 7805–7812. (d) Hasegawa, E.; Nagakura, Y.; Izumiya, N.; Matsumoto, K.; Tanaka, T.; Miura, T.; Ikoma, T.; Iwamoto, H.; Wakamatsu, K. Visible Light and Hydroxynaphthylbenzimidazole Promoted Transition-Metal-Catalyst-Free Desulfonation of *N*-Sulfonylamides and *N*-Sulfonyl-amines. *J. Org. Chem.* **2018**, *83*, 10813–10825.

(19) (a) Hasegawa, E.; Izumiya, N.; Miura, T.; Ikoma, T.; Iwamoto, H.; Takizawa, S.-y.; Murata, S. Benzimidazolium Naphthoxide Betaine is a Visible Light Promoted Organic Photoredox Catalyst. *J. Org. Chem.* **2018**, *83*, 3921–3927. (b) Hasegawa, E.; Tanaka, T.; Izumiya, N.; Kiuchi, T.; Ooe, Y.; Iwamoto, H.; Takizawa, S.-y.; Murata, S. Protocol for Visible-Light-Promoted Desulfonation Reactions Utilizing Catalytic Benzimidazolium Aryloxy Betaines and Stoichiometric Hydride Donor Reagents. *J. Org. Chem.* **2020**, *85*, 4344–4353.

(20) Hasegawa, E.; Yoshioka, N.; Tanaka, T.; Nakaminato, T.; Oomori, K.; Ikoma, T.; Iwamoto, H.; Wakamatsu, K. Sterically Regulated α -Oxygenation of α -Bromocarbonyl Compounds Promoted Using 2-Aryl-1,3-dimethylbenzimidazolines and Air. *ACS Omega* **2020**, *5*, 7651–7665.

(21) (a) Hasegawa, E.; Xu, W.; Mariano, P. S.; Yoon, U. C.; Kim, J. U. Electron-Transfer-Induced Photoadditions of the Silyl Amine, Et₂NCH₂SiMe₃, to α,β -Unsaturated Cyclohexenones. Dual Reaction Pathways Based on Ion-Pair-Selective Cation-Radical Chemistry. *J. Am. Chem. Soc.* **1988**, *110*, 8099–8111. (b) Devadoss, C.; Fessenden, R. W. Picosecond and Nanosecond Studies of the Photoreduction of Benzophenone by *N,N*-Diethylaniline and Triethylamine. *J. Phys. Chem.* **1991**, *95*, 7253–7260. (c) Yoon, U. C.; Mariano, P. S.; Givens, R. S.; Atwater, B. W., III. Photoinduced Electron Transfer Chemistry of Amines and Related Electron Donors. In *Advanced Electron*

Transfer Chemistry; Mariano, P. S., Ed.; JAI Press: Greenwich, 1994; Vol. 4, pp 117–205.

(22) (a) Miyashi, T.; Kamata, M.; Mukai, T. Organic photochemistry. 77. Simultaneous Capture of Two Distinct Radical-Ion Intermediates Generated from the EDA Complexes of Three-Membered Compounds with TCNE by Photoexcitation and in the Dark. *J. Am. Chem. Soc.* **1987**, *109*, 2780–2788. (b) Fukuzumi, S.; Ohkubo, K. Photoinduced Reactions of Radical Ions via Charge Separation. *Encyclopedia of Radicals in Chemistry, Biology and Materials*; John Wiley & Sons, 2012. (c) Kamata, M.; Hagiwara, J.-i.; Hokari, T.; Suzuki, C.; Fujino, R.; Kobayashi, S.; Kim, H.-S.; Wataya, Y. Applications of Triphenylpyrylium Salt-Sensitized Electron-Transfer Photo-Oxygenation Reactions to the Synthesis of Benzo-Fused 1,4-Diaryl-2,3-dioxabicyclo[2.2.2]octanes as New Antimicrobial Cyclic Peroxides. *Res. Chem. Intermed.* **2013**, *39*, 127–137.

(23) Seminal mechanistic investigations of radical anion fragmentation of α -heteroatom substituted acetophenones. (a) Russell, G. A.; Ros, F. Electron transfer processes. 34. Reactions of α -halo ketones with nucleophiles. *J. Am. Chem. Soc.* **1985**, *107*, 2506–2511. (b) Tanner, D. D.; Singh, H. K.; Kharrat, A.; Stein, A. R. The Mechanism of the Reduction of α -Haloketones by Several Models for NADH. Reduction by a SET-Hydrogen Atom Abstraction Chain Reaction. *J. Org. Chem.* **1987**, *52*, 2142–2146. (c) Fukuzumi, S.; Mochizuki, S.; Tanaka, T. Acid-Catalyzed Electron-Transfer Processes in Reduction of α -Haloketones by an NADH Model Compound and Ferrocene Derivatives. *J. Am. Chem. Soc.* **1989**, *111*, 1497–1499. (d) Andersen, M. L.; Mathivanan, N.; Wayner, D. D. M. Electrochemistry of Electron-Transfer Probes. The Role of the Leaving Group in the Cleavage of Radical Anions of α -Aryloxyacetophenones. *J. Am. Chem. Soc.* **1996**, *118*, 4871–4879. (e) Renaud, J.; Scaiano, J. C. Hydrogen vs. Electron Transfer Mechanisms in the Chain Decomposition of Phenacyl Bromides. Use of Isotopic Labeling as a Mechanistic Probe. *Can. J. Chem.* **1996**, *74*, 1724–1730. (f) Andersen, M. L.; Long, W.; Wayner, D. D. M. Electrochemistry of Electron Transfer Probes. Observation of the Transition from Activation to Counterdiffusion Control in the Fragmentation of α -Aryloxyacetophenone Radical Anions. *J. Am. Chem. Soc.* **1997**, *119*, 6590–6595. (g) Andrieux, C. P.; Savéant, J.-M.; Tallec, A.; Tardivel, R.; Tardy, C. Concerted and Stepwise Dissociative Electron Transfers. Oxidability of the Leaving Group and Strength of the Breaking Bond as Mechanism and Reactivity Governing Factors Illustrated by the Electrochemical Reduction of α -Substituted Acetophenones. *J. Am. Chem. Soc.* **1997**, *119*, 2420–2429.

(24) Although some examples of ground state ET and PET promoted reductive desulfonylation of α -sulfonylketones were reported, these reactions were usually performed under the degassed conditions. (a) Fujii, M.; Nakamura, K.; Mekata, H.; Oka, S.; Ohno, A. NAD(P)⁺–NAD(P)H Models. 65. Photochemical Reductive Desulfonylation of β -Keto Sulfones with Hantzsch Ester. *Bull. Chem. Soc. Jpn.* **1988**, *61*, 495–500. (b) Wang, J.; Zhang, Y. The Reductive Desulfonylation of β -Ketosulfones with TiCl₄/Sm System. *Synth. Commun.* **1996**, *26*, 1931–1934. (c) Liu, Q.; Han, B.; Liu, Z.; Yang, L.; Liu, Z.-L.; Yu, W. Photochemical Reductive Desulfonylation of β -Ketosulfones by Ascorbic Acid. *Tetrahedron Lett.* **2006**, *47*, 1805–1807. (d) Yang, D.-T.; Meng, Q.-Y.; Zhong, J.-J.; Xiang, M.; Liu, Q.; Wu, L.-Z. Metal-Free Desulfonylation Reaction Through Visible-Light Photoredox Catalysis. *Eur. J. Org. Chem.* **2013**, *2013*, 7528–7532. (e) Inanaga, K.; Fukuyama, T.; Kubota, M.; Komatsu, Y.; Chiba, H.; Kayano, A.; Tagami, K. Novel and Efficient Chromium(II)-Mediated Desulfonylation of α -Sulfonyl Ketone. *Org. Lett.* **2015**, *17*, 3158–3161.

(25) Reichardt, C. Solvatochromic Dyes as Solvent Polarity Indicators. *Chem. Rev.* **1994**, *94*, 2319–2358.

(26) (a) Sato, T.; Hamada, Y.; Sumikawa, M.; Araki, S.; Yamamoto, H. Solubility of Oxygen in Organic Solvents and Calculation of the Hansen Solubility Parameters of Oxygen. *H. Ind. Eng. Chem. Res.* **2014**, *53*, 19331–19337. (b) Sterckx, H.; Morel, B.; Maes, B. U. W.

Catalytic Aerobic Oxidation of C(sp³)–H Bonds. *Angew. Chem., Int. Ed.* **2019**, *58*, 7946–7970.

(27) As previously discussed,²⁰ HAT between sterically crowded tertiary alkyl radical **7** and bulky hydrogen atom donor **1a** would be difficult to proceed. Thus, although HAT between **7a** and **1a**^{•+} or deprotonated **1a**^{•+} (**17a** in Scheme 4) is expected for the formation of **3a**, it must be also a slow process due to their steric repulsion.

(28) Same LED irradiation of a DMSO (2.0 mL) solution of **1a** (0.15 mmol) and TEMPO (0.10 mmol) in the absence of **2a** under N₂ for 1 h was found to give 1-hydroxy-2,2,6,6-tetramethylpiperidine (TEMPOH) (0.051 mmol, 51%) with the consumption of **1a** (0.058 mmol). TEMPOH: Henry-Riyad, H.; Tidwell, T. T. Thermolysis of N-Tetramethylpiperidinyl Triphenylacetate: Homolytic Fragmentation of a TEMPO Ester. *J. Phys. Org. Chem.* **2003**, *16*, 559–563.

(29) Chauvin, J.-P. R.; Pratt, D. A. On the Reactions of Thiols, Sulfenic Acids, and Sulfinic Acids with Hydrogen Peroxide. *Angew. Chem., Int. Ed.* **2017**, *56*, 6255–6259.

(30) (a) Tolbert, L. M.; Haubrich, J. E. Photoexcited Proton Transfer from Enhanced Photoacids. *J. Am. Chem. Soc.* **1994**, *116*, 10593–10600. (b) Solntsev, K. M.; Huppert, D.; Agmon, N. Solvatochromism of β -Naphthol. *J. Phys. Chem. A* **1998**, *102*, 9599–9606. (c) Tolbert, L. M.; Solntsev, K. M. Excited-State Proton Transfer: From Constrained Systems to “Super” Photoacids to Superfast Proton Transfer. *Acc. Chem. Res.* **2002**, *35*, 19–27. (d) Agmon, N. Elementary Steps in Excited-State Proton Transfer. *J. Phys. Chem. A* **2005**, *109*, 13–35.

(31) According to a reviewer’s suggestion, a deuterium labeling experiment for the photoreaction of **1a** and **2a** was performed using C₂-deuterated **1a-d**. ¹H-NMR analysis of the reaction mixture showed that no sizable deuterium incorporation at α -carbon of **3a** occurred (see Figures S9 and S10), which suggests that HAT from **1a**^{•+} to **7a** would not be mainly operating (path b in Scheme 2). Thus, we tentatively propose that PT from **1a**^{•+} to **2a**^{•-} (path a in Scheme 2) is more likely than (path b) for the formation of **3a**.²⁷

(32) Hasegawa, E.; Tateyama, M.; Hoshi, T.; Ohta, T.; Tayama, E.; Iwamoto, H.; Takizawa, S.-y.; Murata, S. A Photo-Reagent System of Benzimidazoline and Ru(bpy)₃Cl₂ to promote Hexenyl Radical Cyclization and Dowd-Beckwith Ring-Expansion of α -Halomethyl-Substituted Benzocyclic 1-Alkanones. *Tetrahedron* **2014**, *70*, 2776–2783.

(33) Acidity of photo-excited phenol (pK_a = 4, Wehry, E.L.; L. B. Rogers, L. B. Application of Linear Free Energy Relations to Electronically Excited States of Monosubstituted Phenols. *J. Am. Chem. Soc.* **1965**, *87*, 4234–4238) is known to be lower than that of photo-excited 2-naphthol (pK_a = 2.8).^{30a}

(34) Hasegawa, E.; Takizawa, S.; Seida, T.; Yamaguchi, A.; Yamaguchi, N.; Chiba, N.; Takahashi, T.; Ikeda, H.; Akiyama, K. Photoinduced Electron-Transfer Systems Consisting of Electron-Donating Pyrenes or Anthracenes and Benzimidazolines for Reductive Transformation of Carbonyl Compounds. *Tetrahedron* **2006**, *62*, 6581–6588.

(35) Hasegawa, E.; Seida, T.; Chiba, N.; Takahashi, T.; Ikeda, H. Contrastive Photoreduction Pathways of Benzophenones Governed by Regiospecific Deprotonation of Imidazoline Radical Cations and Additive Effects. *J. Org. Chem.* **2005**, *70*, 9632–9635.

(36) Wan, X.; Meng, Q.; Zhang, H.; Sun, Y.; Fan, W.; Zhang, Z. An Efficient Synthesis of Chiral β -Hydroxy Sulfones via Ru-Catalyzed Enantioselective Hydrogenation in the Presence of Iodine. *Org. Lett.* **2007**, *9*, 5613–5616.

(37) Nanjo, K.; Sekiya, M. Formic Acid Reduction. XXVII. Selective Reduction of Carbon–Carbon Double Bonds Conjugated with Nitro and Sulfonyl Groups. *Chem. Pharm. Bull.* **1979**, *27*, 198–203.

(38) Chen, J.; Guo, W.; Wang, Z.; Hu, L.; Chen, F.; Xia, Y. Unexpected Role of p-Toluenesulfonylmethyl Isocyanide as a Sulfonylating Agent in Reactions with α -Bromocarbonyl Compounds. *J. Org. Chem.* **2016**, *81*, 5504–5512.

(39) Fox, D. J.; Pedersen, D. S.; Warren, S. Diphenylphosphinoyl-Mediated Synthesis of Ketones. *Org. Biomol. Chem.* **2006**, *4*, 3102–3107.

(40) Latham, D. E.; Polidano, K.; Williams, J. M. J.; Morrill, L. C. One-Pot Conversion of Allylic Alcohols to α -Methyl Ketones via Iron-Catalyzed Isomerization–Methylation. *Org. Lett.* **2019**, *21*, 7914–7918.

(41) Clerici, A.; Porta, O. Reductive Coupling of Benzoyl Cyanide and Carbonyl Compounds by Aqueous Titanium(III) Ions. A New Convenient and Selective Access to the Less Stable Mixed Benzoin. *J. Org. Chem.* **1993**, *58*, 2889–2893.

(42) Liang, Y.-F.; Wu, K.; Song, S.; Li, X.; Huang, X.; Jiao, N. I_2 - or NBS-Catalyzed Highly Efficient α -Hydroxylation of Ketones with Dimethyl Sulfoxide. *Org. Lett.* **2015**, *17*, 876–879.

(43) Li, Y.; Pouliot, M.; Vogler, T.; Renaud, P.; Studer, A. α -Aminoxylation of Ketones and β -Chloro- α -aminoxylation of Enones with TEMPO and Chlorocatecholborane. *Org. Lett.* **2012**, *14*, 4474–4477.

(44) Sawaki, Y.; Ogata, Y. Kinetics of the base-catalyzed decomposition of α -hydroperoxy ketones. *J. Am. Chem. Soc.* **1975**, *97*, 6983–6989.

(45) Frisch, M. J.; Trucks, G. W.; Schlegel, H. B.; Scuseria, G. E.; Robb, M. A.; Cheeseman, J. R.; Scalmani, G.; Barone, V.; Petersson, G. A.; Nakatsuji, H.; Li, X.; Caricato, M.; Marenich, A. V.; Bloino, J.; Janesko, B. G.; Gomperts, R.; Mennucci, B.; Hratchian, H. P.; Ortiz, J. V.; Izmaylov, A. F.; Sonnenberg, J. L.; Williams-Young, D.; Ding, F.; Lipparini, F.; Egidi, F.; Goings, J.; Peng, B.; Petrone, A.; Henderson, T.; Ranasinghe, D.; Zakrzewski, V. G.; Gao, J.; Rega, N.; Zheng, G.; Liang, W.; Hada, M.; Ehara, M.; Toyota, K.; Fukuda, R.; Hasegawa, J.; Ishida, M.; Nakajima, T.; Honda, Y.; Kitao, O.; Nakai, H.; Vreven, T.; Throssell, K.; Montgomery, J. A., Jr.; Peralta, J. E.; Ogliaro, F.; Bearpark, M. J.; Heyd, J. J.; Brothers, E. N.; Kudin, K. N.; Staroverov, V. N.; Keith, T. A.; Kobayashi, R.; Normand, J.; Raghavachari, K.; Rendell, A. P.; Burant, J. C.; Iyengar, S. S.; Tomasi, J.; Cossi, M.; Millam, J. M.; Klene, M.; Adamo, C.; Cammi, R.; Ochterski, J. W.; Martin, R. L.; Morokuma, K.; Farkas, O.; Foresman, J. B.; Fox, D. J. *Gaussian 16*, Revision C.01; Gaussian, Inc.: Wallingford CT, 2016.

(46) Chai, J.-D.; Head-Gordon, M. Long-Range Corrected Hybrid Density Functionals with Damped Atom-Atom Dispersion Corrections. *Phys. Chem. Chem. Phys.* **2008**, *10*, 6615–6620.

(47) Glendening, E. D.; Reed, A. E.; Carpenter, J. E.; Weinhold, F. *The Gaussian Package Includes the Program of Natural Bond Orbital Analysis: NBO*, version 3.1.

(48) Dennington, R.; Keith, T. A.; Millam, J. M. *GaussView*, version 6; Semichem Inc.: Shawnee Mission, KS, 2016.

(49) *Jmol, an Open-Source Java Viewer for Chemical Structures in 3D*; (Version 14, 2016). <http://www.jmol.org/>.